



DE&S
Duke Engineering & Services



Failed Coating Debris Characterization

Prepared for:

BWROG Containment Coating Committee

Prepared by:

Jan Bostelman and Gilbert Zigler
ITS Corporation

Greg Ashley
Duke Engineering & Services

August 26, 1998



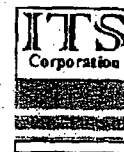
DE&S
Duke Engineering & Services



Executive Summary

This report provides a general classification of the failed coating debris generated by the BWROG Containment Coating Committee autoclave tests conducted in the first part of 1998. A detailed scanning electron microscope analysis of two of the debris types are provided as well as a comparison of mechanical properties of one of the coating debris types with two types of RMI debris.

The failed coating debris from the BWROG autoclave tests are classified into four general categories: (1) large slightly curved pieces, (2) small dimpled pieces, (3) curled pieces, and (4) powder. All debris reviewed had some degree of curvature – no flat debris pieces were noted. The curled paint chips were of a nominal thickness of 200 – 300 μm . The zinc oxide particles ranged in size from 1 μm to 20 μm . The microhardness analysis indicate that the curled paint chips have a KHN of about twice that of a 1.5 mil Aluminum RMI debris simulant and about factor of four less than 2.5 mil Stainless Steel RMI debris.



**BWROG Containment Coating Committee
Failed Coating Debris Characterization**

Table of Contents

Executive Summary ii

1.0 Background: 1

2.0 General Failed Coating Debris Characterization: 1

3.0 Scanning Electron Microscopy (SEM) and Energy Dispersive Spectroscopy (EDS)
Scans of Samples 9C and 12F 6

 3.1 Experimental Set-Up: 6

 3.2 Analysis of Sample 9C (Zinc Oxide Powder): 7

 3.3 Analysis of Sample 12F (Curled Zinc/Epoxy Paint Chip): 13

 3.4 SEM/EDS Analysis Summary: 24

4.0 Microhardness Measurements: 25

 4.1 General Background: 25

 4.2 General Set-Up: 25

 4.3 Microhardness Measurements: 26

 4.4 Calculation of Ultimate Strength Numbers from Microhardness Data 28

 4.5 Microhardness Measurements Summary 28

5.0 References 29



DE&S
Duke Engineering & Services



1.0 Background:

In early 1998 the BWROG Containment Coating Committee conducted a series of autoclave tests with six coating systems on specimens prepared in a manner which would ensure failure (poor surface preparation, excessive thickness, etc.). The specimens were first exposed to a minimum dose of 1.0×10^9 Rads at an average dose rate of 1.65 megarads/hr at the University of Massachusetts Lowell Radiation Laboratory. The specimens were then subjected to a series of three LOCA tests at the Testing Department of Carboline Company. The purpose of the tests was to investigate the post-LOCA failure mechanisms and the failure timing of the coating systems.

On May 1998 the BWROG Containment Coating Committee met and the preliminary results of the autoclave testing were reviewed. Duke Engineering and Services (DE&S) and ITS Corporation offered to the BWROG Containment Coating Committee to characterize the failed coatings debris. This report summarizes the DE&S/ITS characterization of the two main parameters of failed debris coatings needed to estimate the potential head loss of ECCS strainers on BWRs and ECCS recirculation sump screens on PWRs: debris size and shape. Failure mechanisms, failure modes, time to failure and other parameters are addressed and documented elsewhere.

2.0 General Failed Coating Debris Characterization:

The hand-outs of the presentation by Mr. Don Hill at the May 1998 meeting of the BWROG Containment Coating Committee included numerous pictures of tested samples. Visual inspection of these pictures suggests that the failed coating debris can be classified into four broad categories:

- 1) **Large Slightly Curved Pieces:** This debris is represented by essentially all the coating on the coupon coming off as one piece as shown in sample 6B (Figure 1) and sample 12E (Figure 2). The test coupon sizes were 2" x 4" ASTM A36 Steel and 3" x 6" Galvanized Steel. No experimental data was shown for larger coupons, hence it is not known how large a coating debris piece will result. Visual examination of specimen 6B suggests a size of about 3" x 5" inches given that the coupon was Galvanized Steel. The debris would probably have a slight curvature as suggested by the photos.
- 2) **Small Dimpled Pieces:** This is debris that would come from blisters as represented by sample 10E¹ (Figure 3) and 4A (Figure 4). Visual examination suggests blisters ranging in size from 1/16 to 1/4 inch diameter. The debris would be probably be dimpled as suggested by the photos.
- 3) **Curled Pieces:** These are debris that come from curling of pieces of the failed coating as represented by sample 11F (Figure 5). Visual examination suggests curled pieces ranging in length from 1/4 inch to 2 inches and diameters on the

¹ The coupon number on the photograph was hard to see due to blistering. The E was very visible and it appears to have tow digits ahead of the E.



DE&S
Duke Engineering & Services



BWROG Containment Coating Committee Failed Coating Debris Characterization

order of 1/8 inch to 1/4 inch. Sample 12F was provided to ITS Corporation for characterization and the results are reported in sections 3 and 4.

4) **Powder:** This is debris that comes from failed inorganic zinc coating systems as represented by samples 8D (Figure 6). Sample 9C was provided to ITS Corporation for characterization and the results are reported in section 3.

It should be noted that in all cases where the coating failed the coating debris had some degree of curvature, i.e., no flat paint chips were noted.



**BWROG Containment Coating Committee
Failed Coating Debris Characterization**

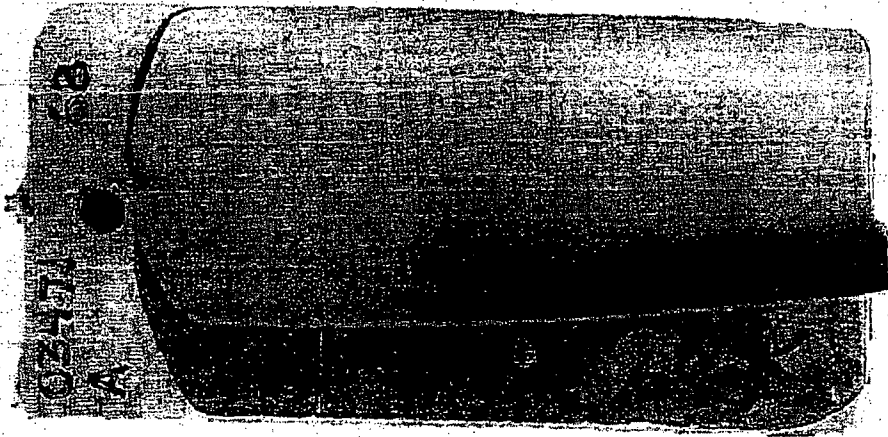


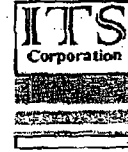
Figure 1: Sample 6B



Figure 2: Sample 12E



DE&S
Duke Engineering & Services



**BWROG Containment Coating Committee
Failed Coating Debris Characterization**



Figure 3: Sample 10E (Note: Assumed Sample ID Number – Poor Picture)

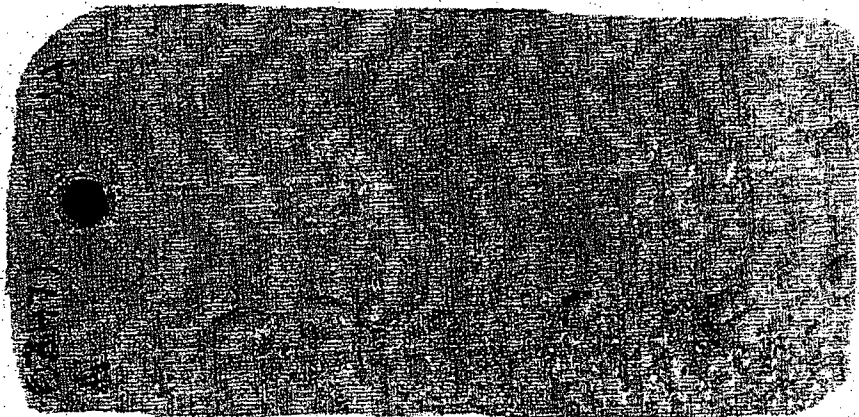


Figure 4: Sample 4A



DE&S
Duke Engineering & Services



**BWROG Containment Coating Committee
Failed Coating Debris Characterization**

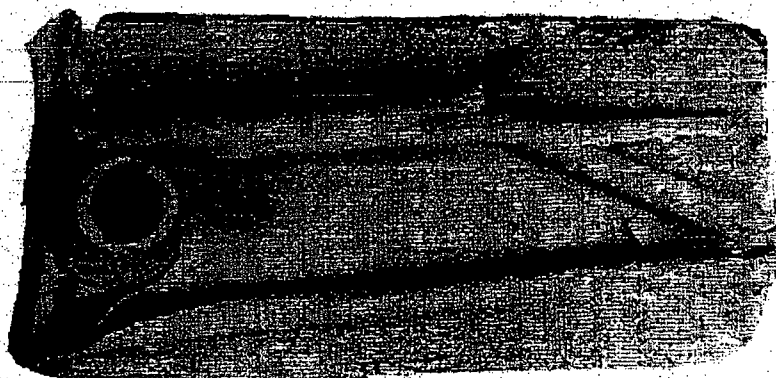


Figure 5: Sample 11F



Figure 6: Sample 8D



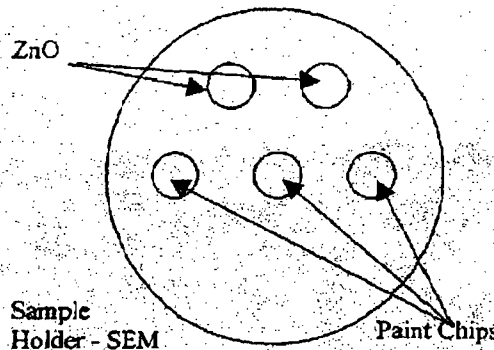
BWROG Containment Coating Committee Failed Coating Debris Characterization

3.0 Scanning Electron Microscopy (SEM) and Energy Dispersive Spectroscopy (EDS) Scans of Samples 9C and 12F

3.1 Experimental Set-Up:

Two samples of failed coatings were received from the BWROG Containment Coating Committee: Samples 9C and 12F. In accordance with Ref. 1, sample 9C is a 1C Carbo Zinc 11 SG system which was irradiated and underwent the LOCA#2 (6 hours LOCA @ 340°F). Ref. 1 indicates that sample 12F is a 2C Carbo Zinc 11 SG over a 1C Carbolite 890 (Blue) system which was irradiated and underwent the LOCA #3 (6 hour LOCA @ 340°F). Scanning Electron Microscopy (SEM) and Energy Dispersive Spectroscopy (EDS) scans of samples 9C and 12F were conducted by J. Bostelman, P.E. Metallurgy-ITS on 6/10/98 at the University of New Mexico Earth and Planetary Sciences department, (JEOL Instrument). The scans were conducted in a low vacuum mode (25-51 mPa), at 20kV, with a typical working distance of 11-16 mm, and stage setting of 10-17 mm. The JEOL was operated in a low vacuum atmosphere (25-51 mPa versus 10^{-7} torr) to enable working with uncoated samples, (otherwise samples would require coating with Gold or Carbon sputtered films). Coating of samples sometimes masks elements of interest when performing EDS scans (especially in polymeric compounds such as epoxy-Carbon based)².

Five samples were mounted for SEM and EDS analysis. Two samples of ZnO powder from sample 9C were mounted loosely on non-conducting tape. Three samples of curled Zn/Epoxy paint chips from sample 12F were mounted on non-conducting tape. The three Zn/Epoxy samples were mounted as such:



1. Paint chip, Zn particle side up, facing the electron beam.
2. Paint chip, Epoxy side up, facing the electron beam.
3. Paint chip, mounted on side, with both epoxy and Zn sides facing electron beam.

The samples were all scanned without interruption on 6/10/98 (hence electron beam variations in current were very minimal). The EDS was not calibrated for a quantitative measurement scan

² See Reference 2.



DE&S
Duke Engineering & Services



BWROG Containment Coating Committee Failed Coating Debris Characterization

with standards, however, the EDS had been recently upgraded and calibrated by the vendor. Eleven digital SEM images were collected, and 6 Polaroid photos were taken during the scanning session. Three EDS scans were collected on the samples for elemental analysis. All scanning was done with a JEOL SEM in the backscattered electron beam mode (BEI), with shadow enhancement on. All digital images were collected with a calibrated signal to enhance the signal to noise ratio, contrast, and brightness. The digital images were collected as ultrafine resolution (512 pixels x 512 pixels), at a medium scan rate, with calibrated scale bar included. Note in SEM analysis, high atomic number elements appear white or light gray, compared to low atomic number elements (such as Carbon) which appear dark gray or black. Zoning of elements can be conducted with EDS scans, but this feature was not utilized across the samples provided.

3.2 Analysis of Sample 9C (Zinc Oxide Powder):

Figure 7 is a low magnification scan of Sample 9C. The powder was loose in a vial, and was applied to a non-conducting tape. The general features indicate predominantly spherical particles of a moderately high atomic number (atomic number > 30).

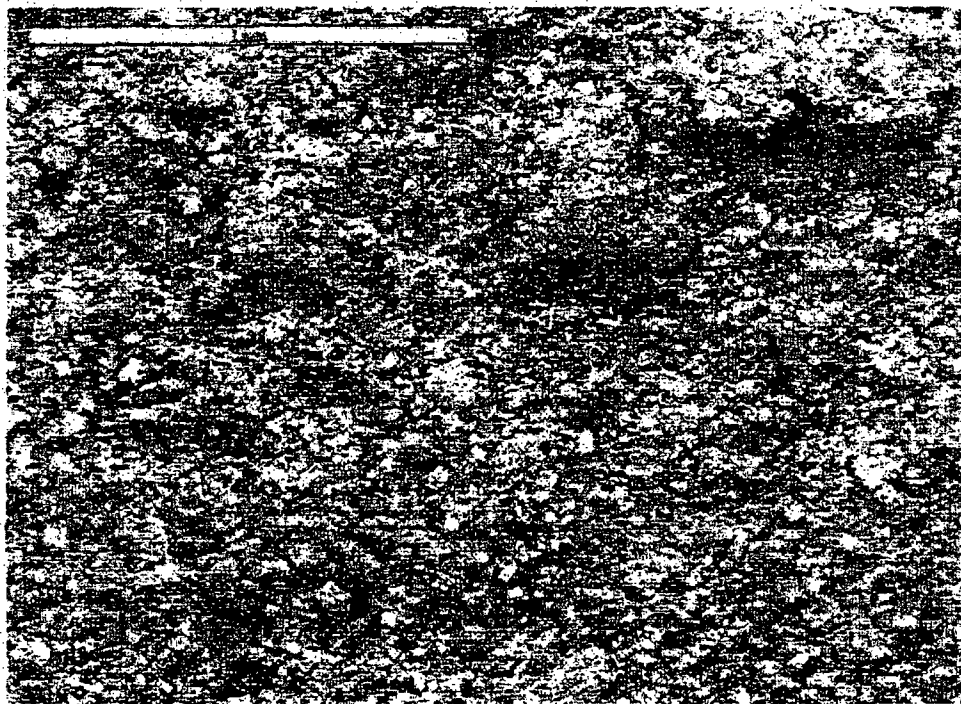


Figure 7: 65X Magnification, 20kV beam, General Surface Features of Zinc Oxide Particles from Sample 9C



**BWROG Containment Coating Committee
Failed Coating Debris Characterization**

Figure 8 is a medium magnification of sample 9C. Note the mixture of large and small particles of ZnO (light colored) with epoxy material (dark colored).

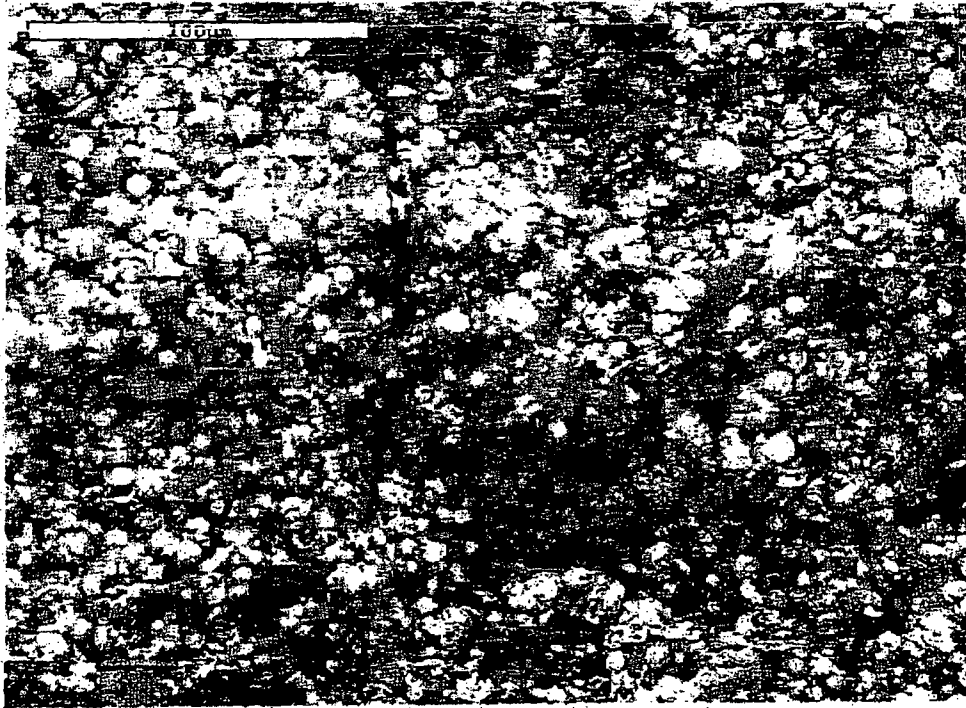


Figure 8: 500X Magnification, 20kV beam, Sample 9C.



**BWROG Containment Coating Committee
Failed Coating Debris Characterization**

Figure 9 is a 1,000 X magnification of sample 9C. The Zinc-Oxide particles are white in color because of the back scattered electron beam used (higher atomic number, 8-9 keV Xray), shadow enhancement capability was turned on. The darker gray matter is most probably epoxy fragments since it is dark in color (low atomic number material, below 1 keV). Note how the larger ZnO particles are fractured and we can not discern if the cleavage fracture lines are along grain boundaries or not at this magnification. The ZnO particles appear to vary in diameter from 1-20µm. The ZnO particle fractures appear similar to ductile failures from overloads (i.e., pressure overloads from within internal structure). The epoxy fragments (thin films) that are visible are thin (less than 1 µm).

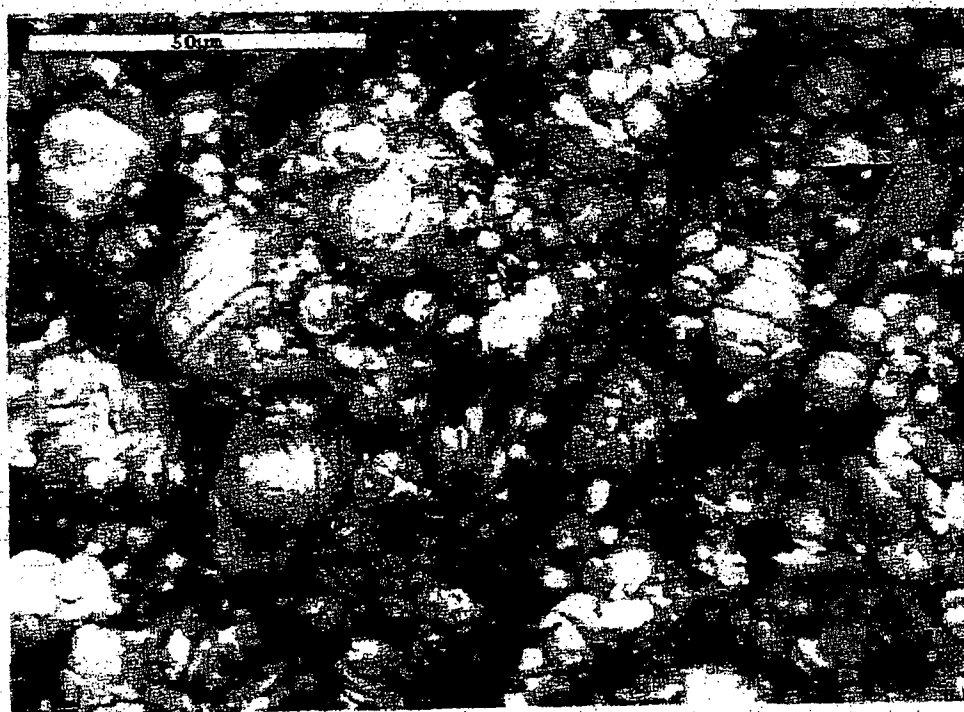


Figure 9: 1,000X Magnification, 20kV beam, Zinc-Oxide Sample 9C



BWROG Containment Coating Committee Failed Coating Debris Characterization

Figure 10 is another image of ZnO particles from a different area of sample 9C and has the same general features of Figure 11. Also note, a large piece of dark material in upper right hand corner, most probably epoxy. The small ZnO particles do not appear to be merely fragments of the larger particles since they are spherical in nature.



Figure 10: 1,000X Magnification, 20kV beam, Sample 9C.



**BWROG Containment Coating Committee
Failed Coating Debris Characterization**

Figure 11 is a high magnification Polaroid photo of sample 9C to obtain a better depth of field. The photo was obtained with a SL3 stored scan (2 minute scan time). a high degree of fracturing in the ZnO particles of 10µm diameter. The fracture surfaces could not be scanned in great detail since working in a low vacuum atmosphere (10^{-7} torr required to get surface relief with Scattered Electron detectors). However, to confirm this, a high vacuum scan would be required, with sputter coating of the sample.

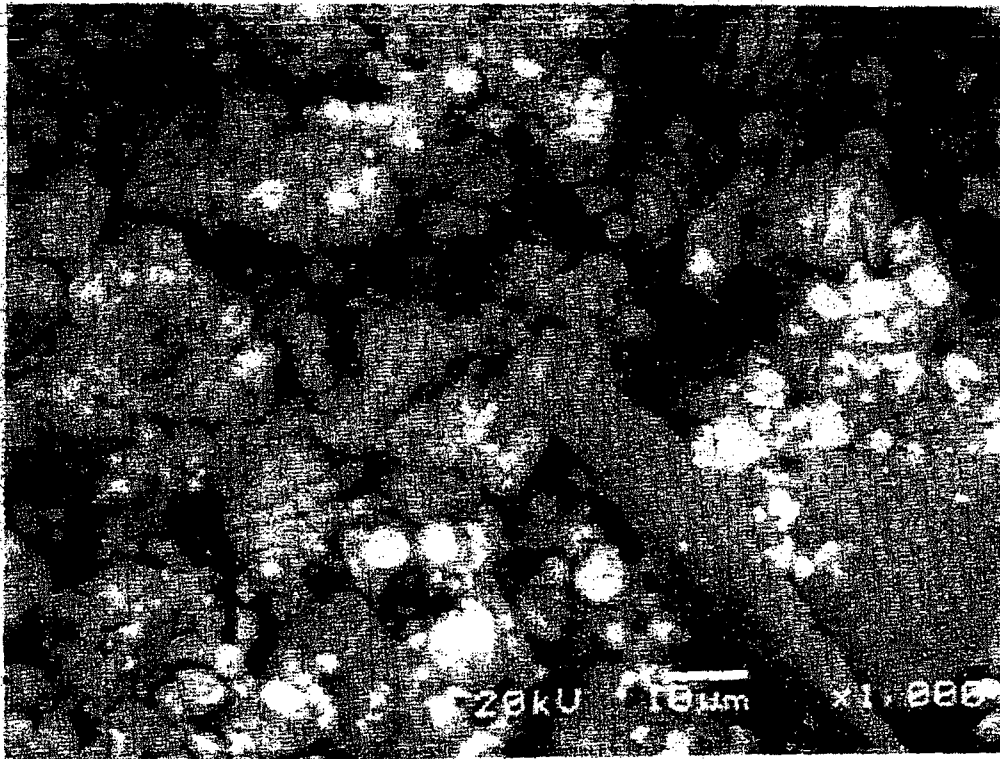


Figure 11: 1,000X Magnification of Sample 9C



**BWROG Containment Coating Committee
Failed Coating Debris Characterization**

Figure 12 is an EDS Scan of sample 9C. Note the relative intensity of Zn with respect to other elements: K, Si, Al, and O. The $K\alpha$, $K\beta$ and L series X-ray lines were exhibited with a high count. The Si could be in the epoxy material or could be a Si escape peak from the detector. The Al and K elements could be impurities in the ZnO powder or epoxy

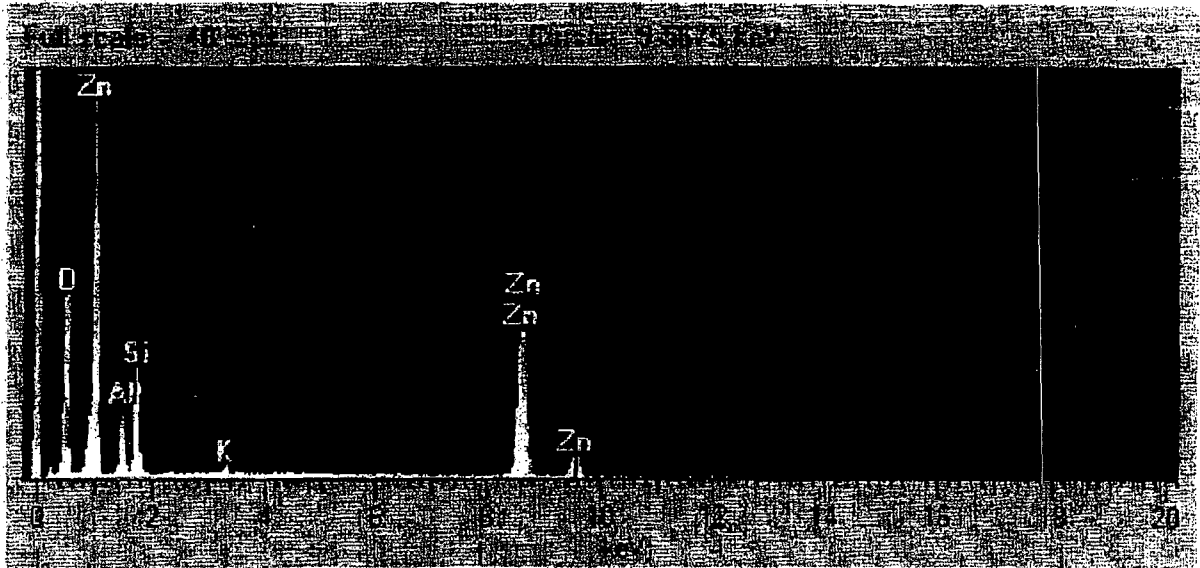


Figure 12: EDS Scan of Sample 9C



BWROG Containment Coating Committee Failed Coating Debris Characterization

3.3 Analysis of Sample 12F (Curled Zinc/Epoxy Paint Chip):

Figure 13 is a low (75X) magnification of one of the curled Zinc/Epoxy paint chip. The edge side of the paint chip was scanned to estimate the thickness of the coating. Note the topside is darker gray than bottom side. The topside is predominantly epoxy with a mixture of a higher atomic number element. The bottom side appears to be a higher atomic number element also. The coating thickness appears to be on the order of 200-300 μ m (average of 275 μ m).

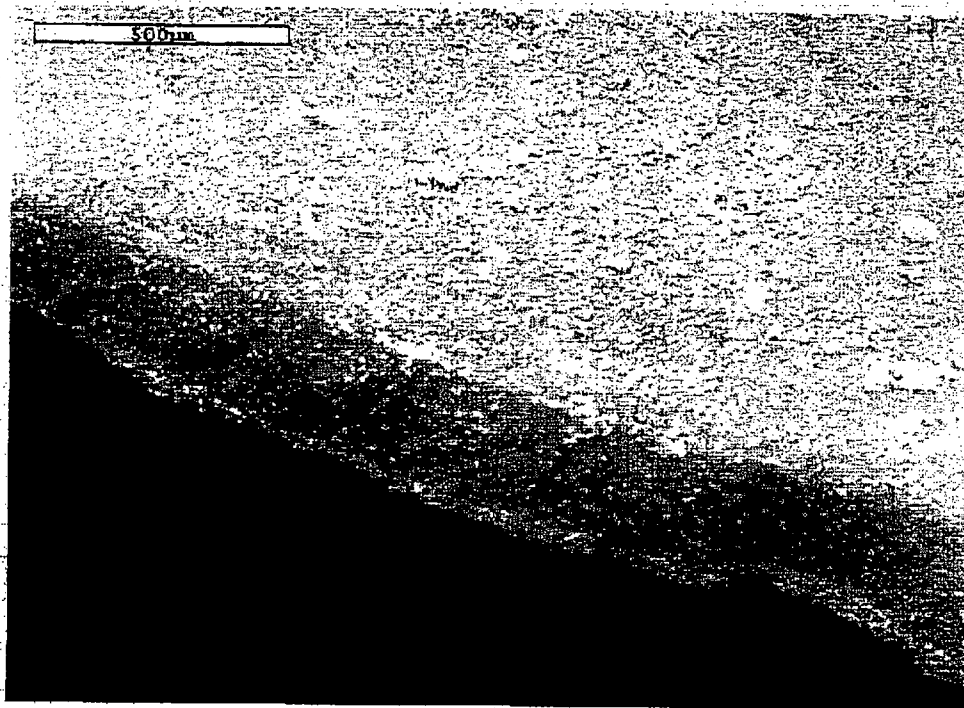


Figure 13: 75X Magnification of a Paint Chip from Sample 12F



**BWROG Containment Coating Committee
Failed Coating Debris Characterization**

Figure 14 is a 75X magnification photo of a paint chip from sample 12F.

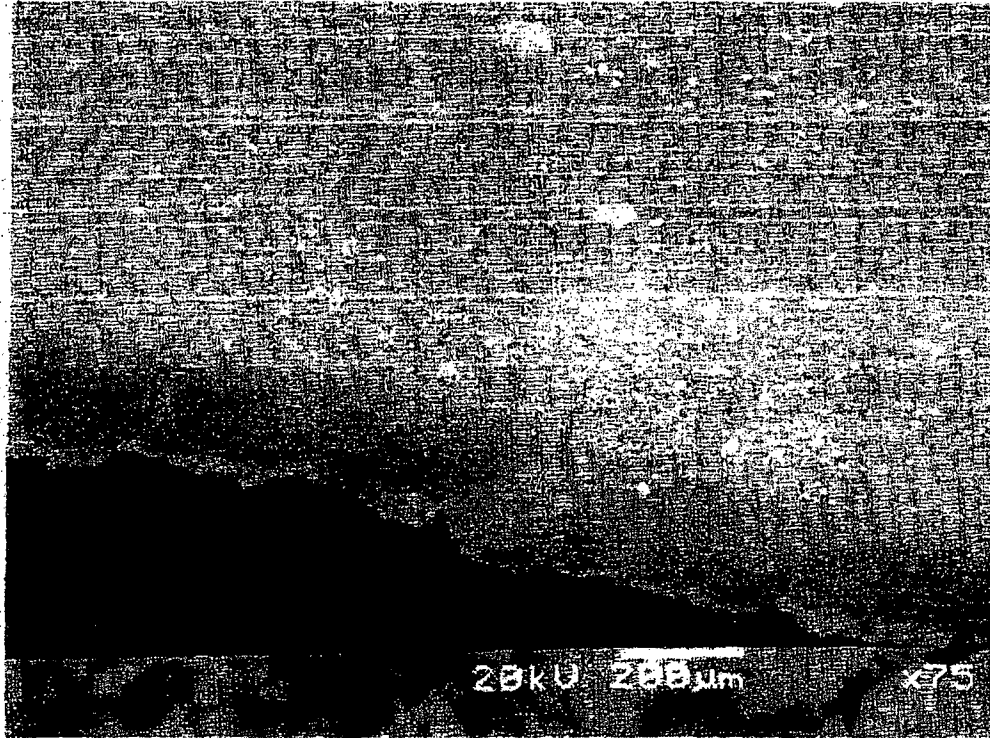


Figure 14: 75X Magnification of an Edge of a Paint Chip from Sample 12F



**BWROG Containment Coating Committee
Failed Coating Debris Characterization**

Figure 15 is a 80X magnification of an edge of a paint chip from sample 12F. Darker layer is the epoxy substrate.

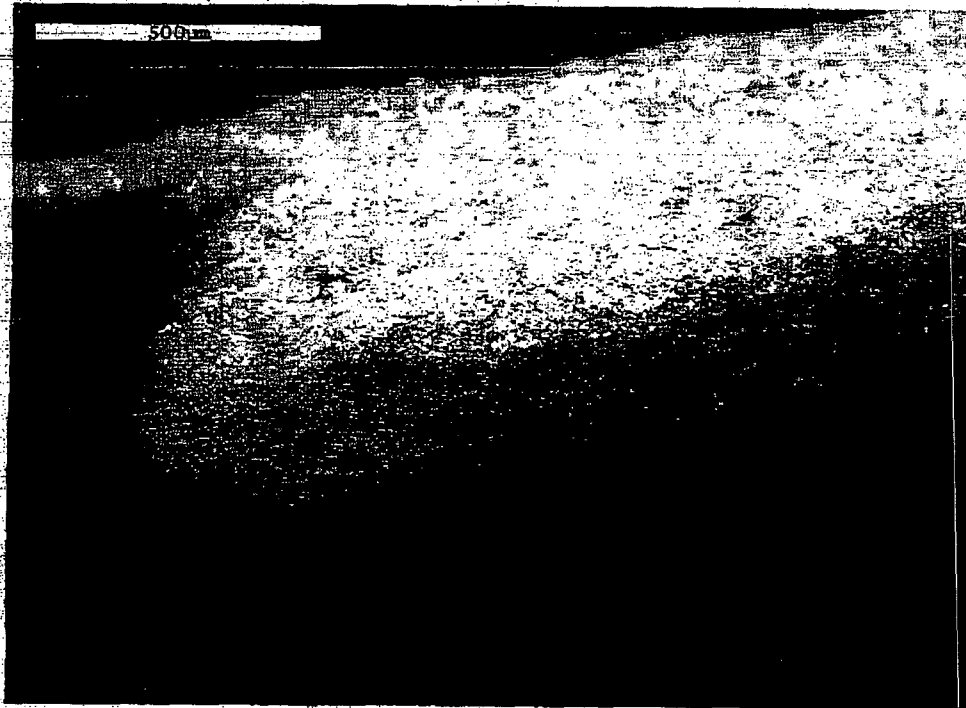


Figure 15: 80X Magnification of an Edge of a Paint Chip from Sample 12F



**BWROG Containment Coating Committee
Failed Coating Debris Characterization**

Figure 16 is a 95X magnification of a paint chip from sample 12F (ZnO side up). Note the epoxy material fragment (darker gray) and the white and spherical ZnO particles.

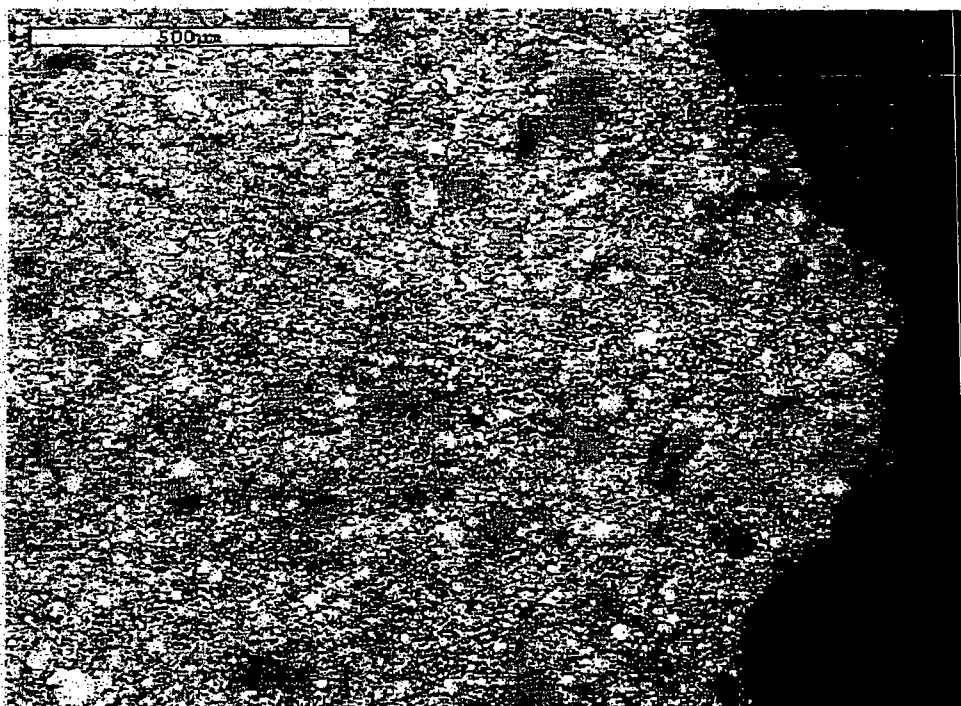


Figure 16: 95X Magnification of Sample 12F ZnO Side Up



**BWROG Containment Coating Committee
Failed Coating Debris Characterization**

Figure 17 is a 220X magnification of an edge of sample 12F paint chip, ZnO side up. Note that there are some particles that are approximately 50um in diameter – possibly agglomerations of smaller particles.

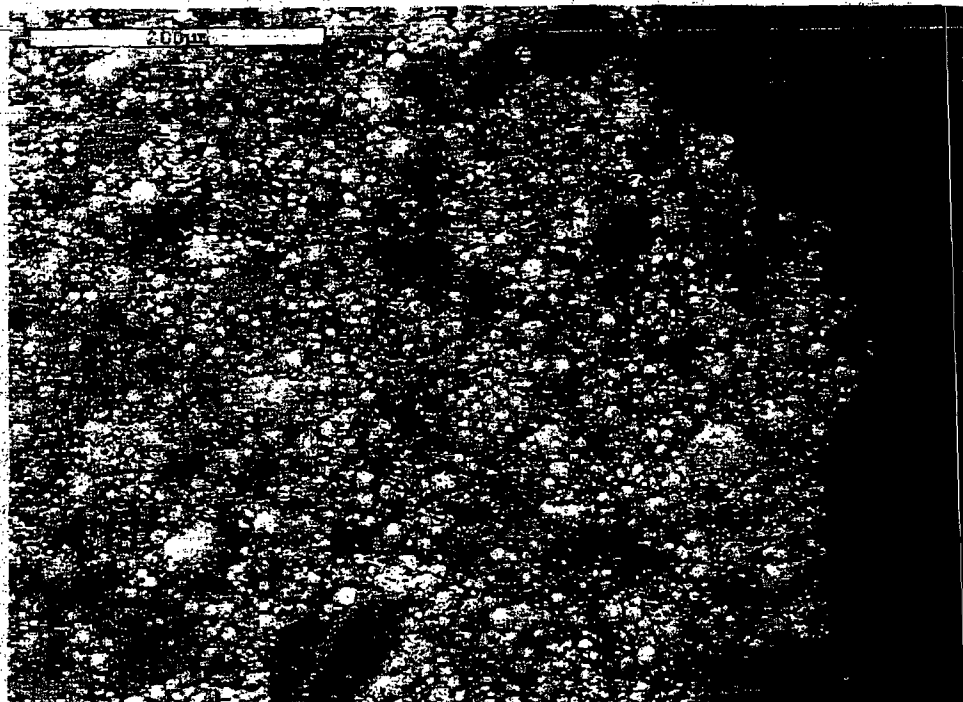


Figure 17: 220X Magnification of an Edge of a Paint Chip from Sample 12F



**BWROG Containment Coating Committee
Failed Coating Debris Characterization**

Figure 18 is a 500X magnification of a paint chip edge from sample 12F. Epoxy layer is the darker layer and the white particles are ZnO.

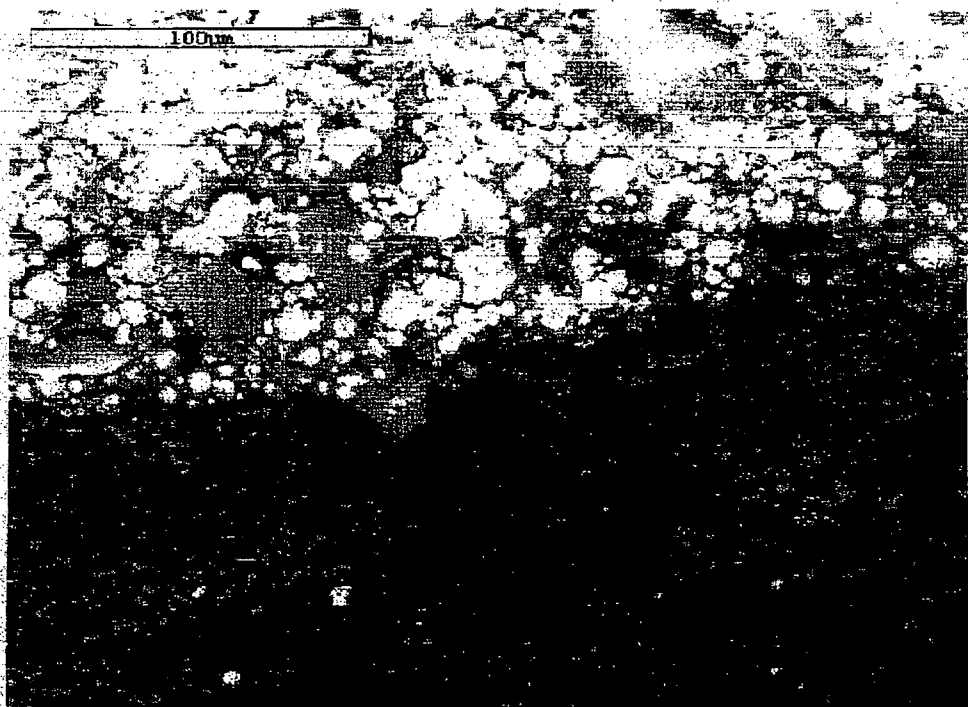


Figure 18: 500X Magnification of an Edge of a Paint Chip from Sample 12F



BWROG Containment Coating Committee Failed Coating Debris Characterization

Figure 19 is a 550X magnification photo of the ZnO side of a paint chip from sample 12F. Note the ZnO particles are primarily intact, not cleaved in half, which would suggest that the epoxy film failed first.

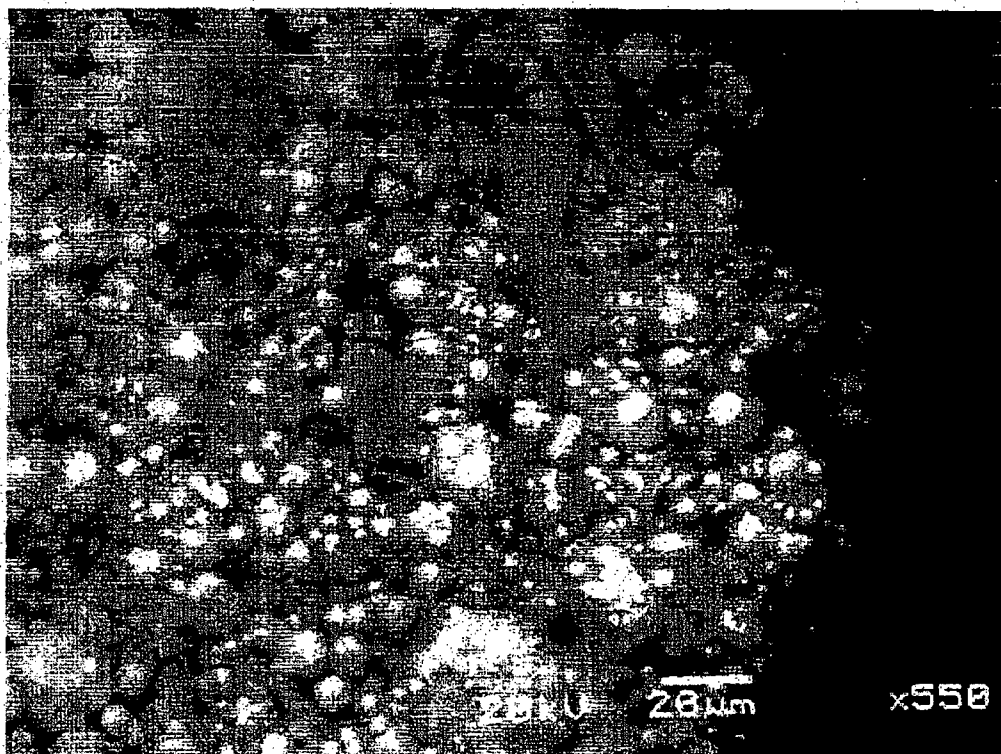


Figure 19: 550X Magnification Photo of the ZnO Side of a Paint Chip from Sample 12F



DE&S
Duke Engineering & Services



**BWROG Containment Coating Committee
Failed Coating Debris Characterization**

Figure 20 is a 2,000X magnification of the ZnO surface of a paint chip from sample 12F. Note that the fractures of ZnO spheres are not as significant as the fractures ZnO of sample 9C.

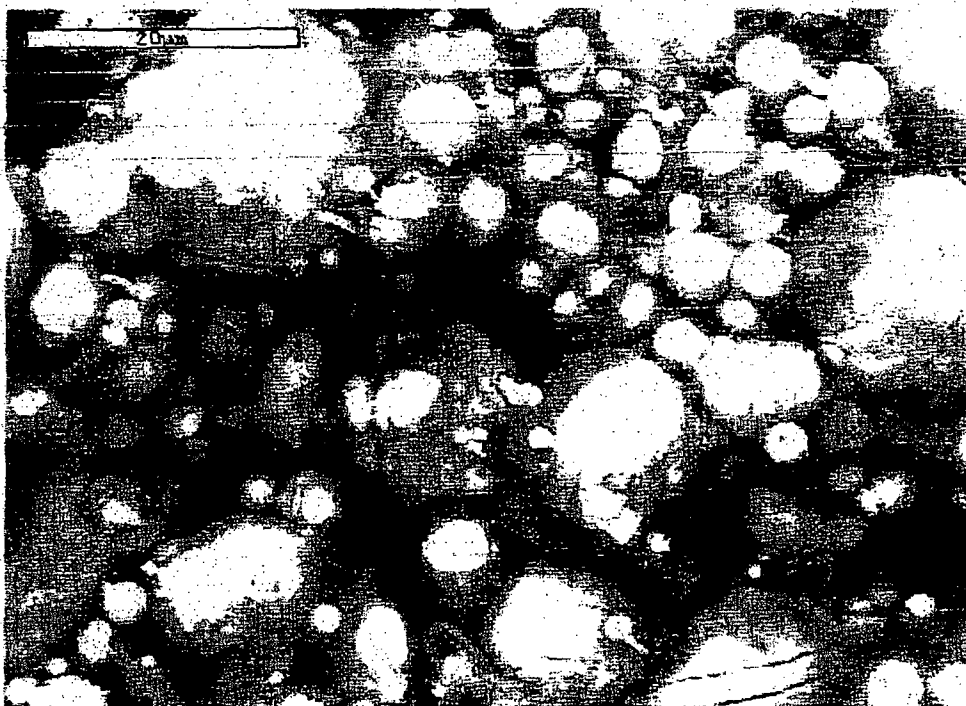


Figure 20: 2,000X Magnification of ZnO Side of a Paint Chip from Sample 12F



**BWROG Containment Coating Committee
Failed Coating Debris Characterization**

Figure 21 is a 2,000X magnification photo of the ZnO side of a paint chip from sample 12F.

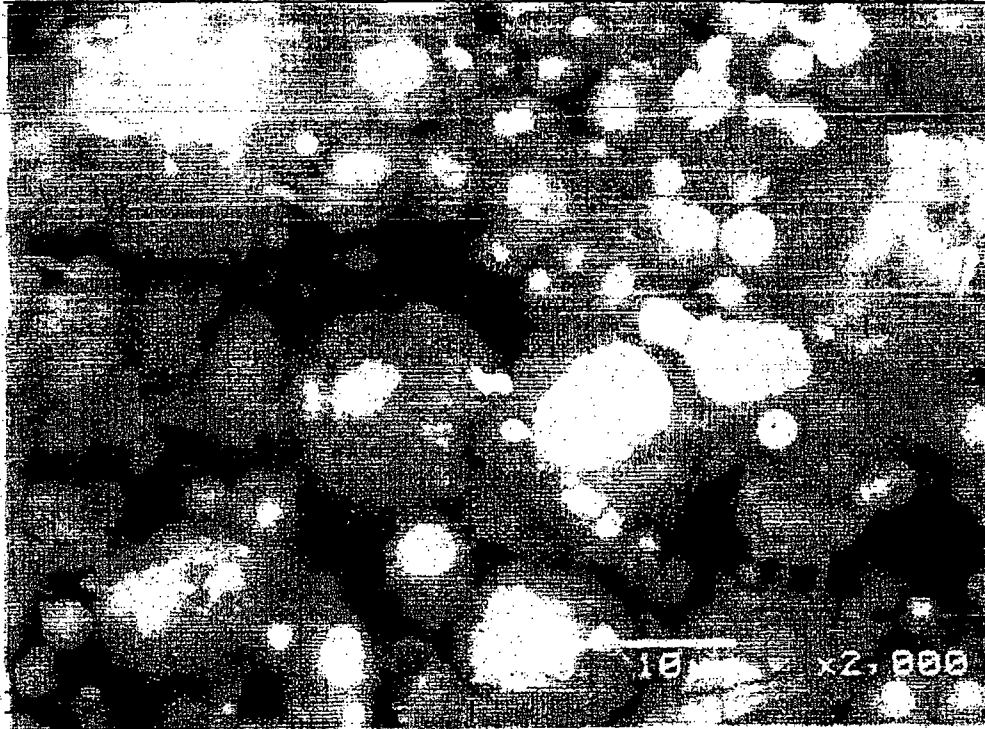


Figure 21: 2,000X Magnification Photo of the ZnO Side of a Paint Chip from Sample 12F.



**BWROG Containment Coating Committee
Failed Coating Debris Characterization**

Figure 22 is a 2,300X magnification photo of the ZnO side of a paint chip from sample 12F. Note the epoxy film around the ZnO particles appearing as "cotton candy" in some areas.

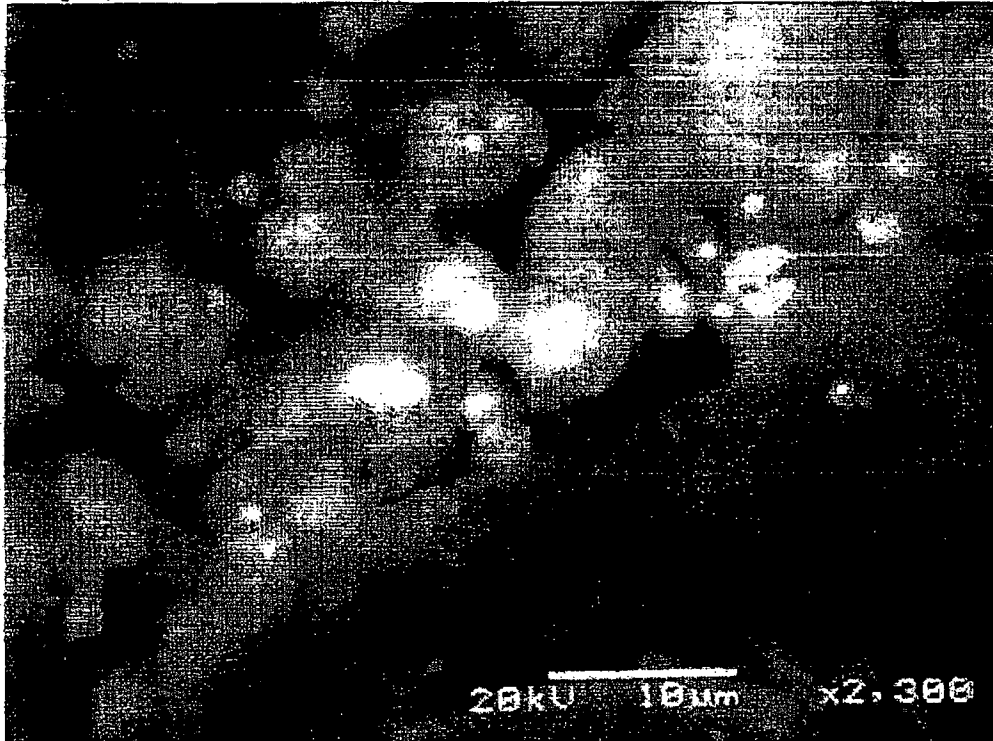


Figure 22: 2,300X Magnification Photo of the ZnO Side of a Paint Chip from Sample 12F



**BWROG Containment Coating Committee
Failed Coating Debris Characterization**

Figure 23 is 3,500X magnification photo of the ZnO side of a paint chip from sample 12F to attempt to look at the fracture surface of the ZnO particles. At these high magnifications focusing is limited by the low vacuum conditions.



Figure 23: 3,500X Magnification Photo of the ZnO Side of a Paint Chip from Sample 12F



BWROG Containment Coating Committee Failed Coating Debris Characterization

Figure 24 is a broad EDS scan of the epoxy side of a paint chip from sample 12F. Note that the paint chip contains Zn, K, Si, Al, O, and C. The In label is probably incorrect; the peak at approximately 3.3 keV is indicative of K K α 1 X-ray line more so than In L series X-ray lines. The only way to absolutely verify the difference is to perform a microprobe wavelength dispersive scan using a microprobe.

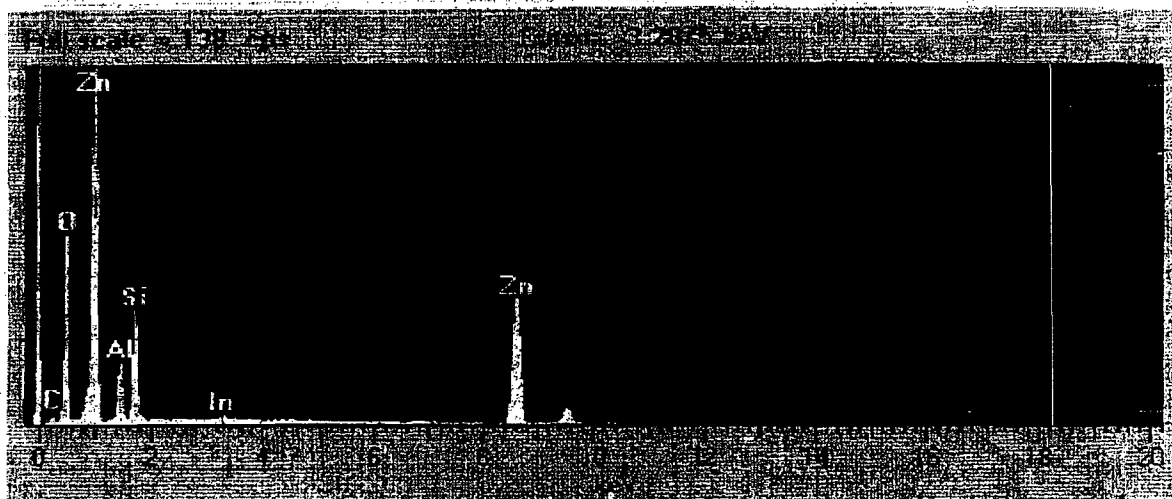


Figure 24: Broad EDS scan at 75X of the Epoxy Side of a Paint Chip from Sample 12F.

3.4 SEM/EDS Analysis Summary:

The following two major conclusions can be drawn from the SEM/EDS efforts on samples 9C and 12F:

1. The ZnO particles of the loose powder from sample 9C ranged in diameter from 1-20 μ m. There were some fragments of thin film epoxy interspersed in the loose powder. The ZnO particles exhibited fractures almost completely through the particle. It could not be determined if the fractures were transgranular or intergranular. Typical brittle fractures are intergranular, e.g., weakening of bond along grain structures.
2. The paint chips from sample 12F appeared to be approximately 200-300 μ m in thickness. The chips have an epoxy rich side and a ZnO rich side. The ZnO particles were of the same size as the loose powder measured from sample 9C (1-20 μ m). The epoxy material appeared to have failed first when examining the ZnO side of the paint chip, since the ZnO particles were primarily intact (except for a few fracture cracks).



DE&S
Duke Engineering & Services



BWROG Containment Coating Committee Failed Coating Debris Characterization

4.0 Microhardness Measurements:

4.1 General Background:

Some of the paint chips from sample 12F were sent to the University of Nebraska-Mechanical Engineering, (Metallurgy Department) for microhardness measurements to obtain insights as to the resistance of the paint chips to deformation loads. Hardness measurements can also relate to the strength and heat treatment of a material. Dr. William Weins and Dr. John Makinson of the University of Nebraska conducted the microhardness measurements of the paint chip samples with a Knoop diamond indenter. Dr. Weins is a noted specialist in metallurgy and micro system measurements.

Microhardness measurements were performed since the paint chips are relatively small in comparison to sample sizes required for full-scale ASTM hardness or tensile strength testing. In addition microhardness measurements can be empirically correlated to the yield strength of the material. However, note that hardness conversions are empirical relationships. Since the elastic moduli are not known for the paint coating, it will be difficult to correlate exactly the microhardness readings of this material to ultimate strength values such as can be done for well tested materials such as stainless steel or aluminum. Microhardness measurements are relatively non-destructive with very little indentation seen visually on the surface of the material. Some strain hardening of the epoxy may occur during the loading of the diamond indenter during the tests. However, for comparison purposes the raw values from the Knoop indenter tests were taken and correlated to ultimate strength values.

For comparison of the paint chip microhardness measurements, two different debris samples of reflective metal insulation (RMI) foil were also sent for microhardness testing. One RMI debris sample was a 2.5 mil Stainless Steel foil debris that came from the Karlshamn full scale debris generation tests conducted at the Siemens-KWU facility in Germany by the Nuclear Regulatory Commission. The other RMI debris sample was a piece of 1.5 mil Aluminum RMI debris simulant. The Al RMI debris simulant was made from the same type of Aluminum foil stock material used to manufacture Al RMI insulation, sized and crumbled to have the same appearance as the Siemens-KWU generated RMI debris.

4.2 General Set-Up:

The 0.2 percent offset yield strength of materials can be determined with good precision from Vickers hardness measurements according to the relation (Ref. 3)

$$\sigma_o = (DPH/3) (0.1)^{n'-2}$$

σ_o = the 0.2 percent offset yield strength, kg/mm²

DPH = Vickers hardness number

$n' = n + 2$ = the exponent in Meyer's law

n' is typically 2 - 2.5 for annealed to strain hardened materials (Ref. 3), if the value of 2 is input, then the equation for 0.2 percent offset yield strength is



**BWROG Containment Coating Committee
Failed Coating Debris Characterization**

$$\sigma_o = (DPH/3)$$

if $n^2 = 2.5$ then the equation is as follows

$$\sigma_o = (DPH/3) (0.1)^2$$

For purposes of comparison it was assumed that the Knoop Indenter hardness numbers are equivalent to Vicker's Diamond Hardness numbers. However, it should be noted that the Knoop and Vicker's measurements vary in size of the indentation. Knoop indenters can place indentations much closer together than with square Vickers indentations, and only require 15% of the indentation depth and area as Vickers measurements.

The Knoop Hardness numbers are recorded in kg/mm^2 , and are determined as follows:

$$KHN = P/L^2 C$$

Where,

KHN = kg/mm^2 ,

P = applied load in kg,

L = length of long indentation diagonal in mm,

C = constant for the indenter, supplied by manufacturer,

Drs. Weins and Makinson used a Standard to evaluate the Knoop hardness loadings prior to performing the testing on the samples. The standard hardness readings are as follows:

Load = 500 g

Standard 455 +/- KHN

Load	Readings	
		KHN
500g		448
100g		566
100g		576

Thus, the standard reading at 500g loading was within the standard block readings

4.3 Microhardness Measurements:

Table 1 are the results of microhardness measurements for a paint chip from sample 12F, Table 2 documents the results of the Al RMI debris simulat, and table 3 the results for the Stainless Steel RMI debris.

Table 1 - Microhardness Measurements Paint Side Up

Reading	FU	Microns - L	KHN
1	603	148.88	64
2	680	167.89	50
3	622	153.57	60
4	568	140.24	72

Average = 61.84 KHN

Standard Deviation = 9.08 KHN



**BWROG Containment Coating Committee
Failed Coating Debris Characterization**

Table 2 – Microhardness Measurements Aluminum Foil

Reading	FU	Microns - L	KHN
1	443	272.27	19
2	358	220.03	29
3	357	219.41	30
4	375	230.48	27
5	374	229.86	27
6	413	253.83	22
7	439	269.81	20
8	387	237.85	25
9	343	210.81	32
10	293	180.08	44

Average = 27.45 KHN
Standard Deviation = 7.18 KHN

Table 3 – Microhardness Measurements of Stainless Steel Foil

Reading	FU	Microns - L	KHN
1	293	72.34	272
2	292	72.09	274
3	272	67.16	315
4	276	68.14	306
5	273	67.4	313
6	261	64.44	343
7	259	63.95	348
8	271	66.91	318
9	322	79.5	225
10	285	70.37	287

Average = 300.17 KHN
Standard Deviation = 36.72 KHN



**BWROG Containment Coating Committee
Failed Coating Debris Characterization**

4.4 Calculation of Ultimate Strength Numbers from Microhardness Data

Assuming that the KHN readings are equivalent to DPH we can use the equations noted previously:

$n' = 2.0$ then the equation is as follows

$$\sigma_o = (DPH/3)$$

$n' = 2.5$ then the equation is as follows

$$\sigma_o = (DPH/3) (0.1)^5$$

Table 4 – 0.2% Yield Strength Correlation for $n' = 2.0$ and 2.5

n' Material	Standard Block (ksi)	Paint Chip (ksi)	Aluminum Foil (ksi)	Stainless Steel Foil (ksi)
$n' = 2.0$	212	29	13	142
$n' = 2.5$	67	9	4	45

Assuming that the Stainless Steel Foil is 304 type, the 0.2% offset yield strengths of this material are 36 ksi (0% cold worked) to 145 ksi (60% cold worked) Ref. 4. Thus, the values calculated above are within this range for Type 304 Stainless Steel. Since the material was formed by rolling process, and then subjected to a steam jet blast, it is anticipated that a significant amount of cold working has occurred in the sample. Therefore, the value of 142 ksi for a measurement of 0.2% Yield Strength is conceivable.

For Aluminum Sheets, the 0.2% Yield Strength of various alloys and tempering was found to be as low as 11 ksi (Type 5154) to a maximum of 59 ksi (Alclad 2014-T6) Ref. 5. The reading of 13 ksi calculated from the previous equations would fit this range. Thus, from the readings one could gage that the correlation with an n' fit of 2.0 best represents known properties of the metallic foils. Given this, the paint chip material then could be correlated to have a 0.2% Yield Offset Strength of 29 ksi.

4.5 Microhardness Measurements Summary

The tests results indicate that the Stainless Steel RMI debris had the highest microhardness numbers (300.17 KHN) (resistance to the indenter) than the paint chip of sample 12F and Al RMI debris simulant (61.84 KHN, 27.45 KHN respectively). Given assumptions that the KHN numbers are equal to DPH numbers then the resulting 0.2% Yield Offset Strengths were calculated:

- Paint Chip³ – 29 ksi
- Aluminum Foil – 13 ksi
- Stainless Steel – 142 ksi

³ Assumes very little strain hardening.



BWROG Containment Coating Committee Failed Coating Debris Characterization

5.0 References

1. LOCA Coating Testing, Determining the Point of Failure During a 340F DBA/LOCA, Don Hill, April 5, 1998
2. Scanning Electron Microscopy and X-Ray Microanalysis, A Text for Biologists, Materials Scientists, and Geologists, 2nd Edition, Goldstein, Joseph I., et al, Plenum Press, 1992.
3. Mechanical Metallurgy, Dieter, George E., McGraw-Hill Book Company, 2nd Edition, 1976, pgs. 389-402.
4. Structure and Properties of Engineering Alloys, Smith, McGraw-Hill Book Company, 1st Edition, 1981, pg. 302.
5. Aluminum Construction Manual, the Aluminum Association, 1st Edition, 1959, pgs. 291-295.
6. Juhani Hyvarinen and Olli Hongisto, "Metallic Insulation Transport and Strainer Clogging Tests", STUK, Finnish Centre for Radiation and Nuclear Safety, July 1994

Corrected Replacement Pages to Enclosure of
Supplemental Response to Generic Letter 2004-02, "Potential Impact of Debris Blockage on
Emergency Recirculation during Design Basis Accidents at Pressurized Water Reactors,"
dated February 29, 2008 (LIC-08-0021)

Mark-ups and Retyped "Clean" Pages

(51 total pages)

- Notes: (1) The clean pages supersede their respective pages provided in the February 29, 2008, response letter.
- (2) The pagination of the markup pages does not align with the original letter due to deletion and addition of text. This is corrected in the clean pages.

1. Overall Compliance

Fort Calhoun Station (FCS) will be in compliance with the regulatory requirements listed in the Applicable Regulatory Requirements section of Generic Letter (GL) 2004-02 upon completion of the upcoming refueling outage (RFO) currently scheduled for May 24, 2008.

The Applicable Regulatory Requirements section of NRC Generic Letter (GL) 2004-02 states:

NRC regulations in Title 10, of the Code of Federal Regulations Section 50.46, 10 CFR 50.46, require that the ECCS have the capability to provide long term cooling of the reactor core following a LOCA. That is, the ECCS must be able to remove decay heat, so that the core temperature is maintained at an acceptably low value for the extended period of time required by the long lived radioactivity remaining in the core.

Similarly, for PWRs licensed to the General Design Criteria (GDCs) in Appendix A to 10 CFR Part 50, GDC 38 provides requirements for containment heat removal systems, and GDC 41 provides requirements for containment atmosphere cleanup. Many PWR licensees credit a CSS, at least in part, with performing the safety functions to satisfy these requirements, and PWRs that are not licensed to the GDCs may similarly credit a CSS to satisfy licensing basis requirements. In addition, PWR licensees may credit a CSS with reducing the accident source term to meet the limits of 10 CFR Part 100 or 10CFR50.67. GDC 35 is listed in 10CFR50.46(d) and specifies additional ECCS requirements. PWRs that are not licensed to the GDCs typically have similar requirements in their licensing basis.

Exceptions to the applicable regulatory requirements of GL 2004-02 for FCS are as follows:

The Omaha Public Power District (OPPD) License Amendment Request (LAR) 07-04 (Reference 16) was submitted to the NRC for approval of a change in the containment spray system (CSS) actuation logic, which will eliminate automatic containment spray initiation for a loss-of-coolant accident (LOCA). Following NRC approval, FCS will **no** longer credit the CSS for heat removal capacity or for iodine removal post-LOCA. The CSS will continue to actuate during a main steam line break (MSLB), which does not require use of safety injection pumps in the recirculation mode. Compliance with the regulatory requirements of GL 2004-02 is based on NRC approval of the LAR by April 1, 2008, so that the proposed changes can be implemented during the 2008 RFO.

Compliance will be achieved through analysis, plant specific testing, larger sump strainers installed in 2006, implementation of LAR-07-04 removing containment spray (CS) for containment pressure mitigation during a LOCA as part of water management initiative strategies, completed plant modifications that reduce debris, and associated programmatic and process changes to ensure continued compliance.

will be lower than the available net positive suction head (NPSH) **margin**. The results of testing demonstrate that the FCS strainer design is capable of operating under both LBLOCA and SBLOCA scenarios without generating a vortex, which would result in the entrainment of air into the strainers and the emergency core cooling system (ECCS).

The revised containment spray configuration will maintain post-LOCA core injection and required flow through the containment sump strainer while minimizing the bulk containment sump pool debris transport.

For NPSH margin calculations refer to detailed assessments provided in Section 3.g.

Programs are in place to control insulation and coatings inside containment. Controls include inspections of containment coatings each RFO and assessment and engineering evaluation prior to changeout or removal of insulation. Configuration control checklists exist (See OPPD response to 3i) that require prior evaluation of any changes to the amount of aluminum in containment.

FCS has undergone extensive containment cleaning programs since 2003 including the major component replacement projects (SG, PZR and RPV head) of the 2006 RFO. Containment closeout and foreign material exclusion programs ensure that debris is monitored or controlled within design limits.

In conclusion, OPPD is taking the appropriate actions in response to GL 2004-02 to ensure acceptable ECCS performance in the recirculation mode. With the completed actions (i.e., new sump strainers, replacement of sump buffering agent, insulation removal), detailed analyses and testing, and implementation of the modification to CSS actuation logic following NRC approval of LAR-07-04, OPPD is in compliance with the requirements of GL 2004-02. Long-term programs for control and monitoring of debris will ensure that the ECCS will continue to conform to the requirements of GL 2004-02.

Remaining actions outlined in this response required to address the issues in GL 2004-02 will be completed by the dates established between OPPD and the NRC. The configuration of the plant that will exist once all 2008 RFO modifications and actions are implemented for regulatory compliance is discussed next.

Filter Media – Charcoal & Fiberglass

NEI 04-07 (Reference 48) has insufficient data or direction regarding the destruction pressures or debris size distribution of generic low-density fiberglass. Absent applicable experimental data, a value of 100% small fines is adopted by this analysis for filter media in a ZOI. Per the walkdown packages, no filter media is located within the bioshield and is therefore not subject to debris generation as a result of a LOCA. All of the charcoal media is located on the operating floor elevation of 1060' and all of the fiberglass media is on the 1060' elevation or outside the bioshield. This filter media is outside of any ZOI and is not subject to direct containment spray impingement; therefore, filter media is not considered a credible debris source.

Pabco® HD Supertemp (Calcium Silicate) Fire Barrier Board Panel

Absent applicable experimental data, a value of 100% small fines is adopted by this analysis for Pabco® HD Supertemp in a ZOI. Per the walkdown packages, no Pabco® HD Supertemp is located within the bioshield and is therefore not subject to debris generation as a result of a LOCA.

Fiberglass – E-glass Installed at Inlet Nozzles of Reactor Vessel

Approximately 150 feet of fiberglass rope have been installed at the inlet nozzles of the reactor vessel to fill gaps in an effort to reduce heat losses. This is the only fibrous debris source in the case of a reactor vessel nozzle break.

Break No. 1 – Largest Potential for Debris

The LBLOCA in the RCS is the controlling break in terms of quantity of debris generated. The quantities of debris source material are distributed in the FCS containment as follows:

**Table 5
 Insulation Quantity by Location**

Insulation Type	Inside Bio-shield	Outside Bio-shield	Total
Asbestos (ft ³)	353.11	358.35	711.46
Calcium Silicate (ft ³)	16.68	33.20	49.88
Cerafiber (ft ³)	2.35	1.93	4.28
Fiberglass (ft ³)	381.86	969.97	1351.83
Foam Rubber (ft ³)	0.97	11.08	12.05
NUKON® (ft ³)	4.73	16.24	20.96
Pabco® HD Supertemp (ft ³)	0.00	12.69	12.69
Phenolic Bonded Glass Fiber (ft ³)	0.00	800.00	800.00
Temp-Mat® (ft ³)	189.90	43.92	233.82
RMI (ft ²)	105483.98	0.00	105483.98

Given the arrangement of the RCPs and steam generators (SGs), a fully offset double-ended guillotine break (DEGB) in the hot leg just prior to the vertical rise would most likely destroy the maximum amount of insulation. A 32-inch break of piping (hot leg)

**Table 6
Break No. 1 LBLOCA**

Debris Type	Debris Size	Debris Quantity Generated (ft ³)			
		RC-2A Hot Leg SG A Bay	RC-3A Cold Leg SG A Bay	RC-2B Hot Leg SG B Bay	RC-3D Cold Leg SG B Bay
Stainless Steel RMI (ft ²)	Fines (<0.25")	9931.80	9931.80	9931.80	9931.80
	Small Pieces (<4")	19863.60	19863.60	19863.60	19863.60
	Large Pieces (>4")	3310.60	3310.60	3310.60	3310.60
	Total	33106.00	33106.00	33106.00	33106.00
TempMat® (ft ³)	Fines	9.51	7.44	5.38	0.96
	Small Pieces (<6")	37.01	29.55	21.13	3.71
	Large Pieces (>6")	33.16	6.76	13.10	4.40
	Intact Pieces (>6")	35.23	7.18	13.91	4.67
	Total	114.91	50.93	53.52	13.75
LDFG - NUKON® (ft ³)	Fines	0.04	0.02	0.65	0.11
	Small Pieces (<6")	0.18	0.02	2.68	0.09
	Large Pieces (>6")	0.00	0.09	0.57	0.55
	Intact Pieces (>6")	0.00	0.10	0.60	0.59
	Total	0.22	0.22	4.51	1.34
LDFG - Fiberglass (ft ³)	Fines	20.96	10.72 11.10	19.16	11.63
	Small Pieces (<6")	70.73	34.65 36.08	72.10	39.99
	Large Pieces (>6")	21.77	18.97 18.09	8.32	18.55
	Intact Pieces (>6")	23.35	20.31 19.37	8.92	19.83
	Total	136.78	84.64	108.50	89.99
Cal-Sil (ft ³)	Particulate	2.48	0.16	0.61	0.03
	Pieces > 1"	2.48	0.11	0.40	0.02
	Total	4.96	0.27	1.01	0.06
Cal-Sil (w/ Asbestos) (ft ³)	Particulate	21.67	8.68	22.91	20.02
	Pieces > 1"	17.46	6.15	15.03	16.73
	Total	39.13	14.83	37.94	36.75
Cerafiber (ft ³)	Total (Fines)	0.63	0.63	1.72	1.72
Foam Rubber (ft ³)	Total (Fines)	0.54	0.54	0.43	0.43
Sand (ft ³)	Total (Fines)	0.00	0.00	0.00	0.00

The quantity of RMI insulation destroyed is very conservative as the destruction pressure for RMI is much higher than that of fibrous insulation and would equate to a much smaller ZOI. However, this conservative result has little impact on sump screen performance compared to the effects of the fibrous insulation, as the transport analysis will show.

Break No. 2 – Large breaks with two or more different types of debris

Break No. 1 has the largest amount of insulation and has several different types of debris. Therefore, the debris generation of Break No. 1 envelopes that of Break No. 2. The intent of Break No. 2 is to ensure that the analysis considers breaks with the potential to transport a variety of debris types. For example, a break with fiber and particulate debris could result in higher head loss across the sump screen than a break with only fiber, even if the latter break produces a much greater quantity of fiber. Since the Break No. 1 cases all generate a variety of debris types (high-density fiber, low-

bay area, and on the left side of Figure 6 is the B SG bay area. The bay areas are not connected to each other at the basement floor elevation, hence water or debris that is generated in one bay area cannot flow or transport directly to the other one. There are two distinct entrances to the bay areas. Each entrance has a key locked chain link fence type door. There are gaps at the bottom of each screened door and on the sides (5" x 38"). **In addition, Given the size of these openings, it is not likely that debris would block the openings sufficiently to prevent water from reaching the sump. the doors are locked open during power operations, therefore water from the SG bays is not prevented from reaching the sump strainers.** The depth of the FCS sump pool is fairly significant (at least 4'). ~~For any debris trapped at the bottom of the chain link door, water would flow over the top of the debris.~~ The entrance to the reactor cavity is not inside these bay areas, any water entrained with debris that would get to the reactor cavity shaft would not be held up and would spill over.

Blockage in the refueling canal is not an issue for FCS; with a no-spray configuration there will not be any significant water flow into the refueling canal.

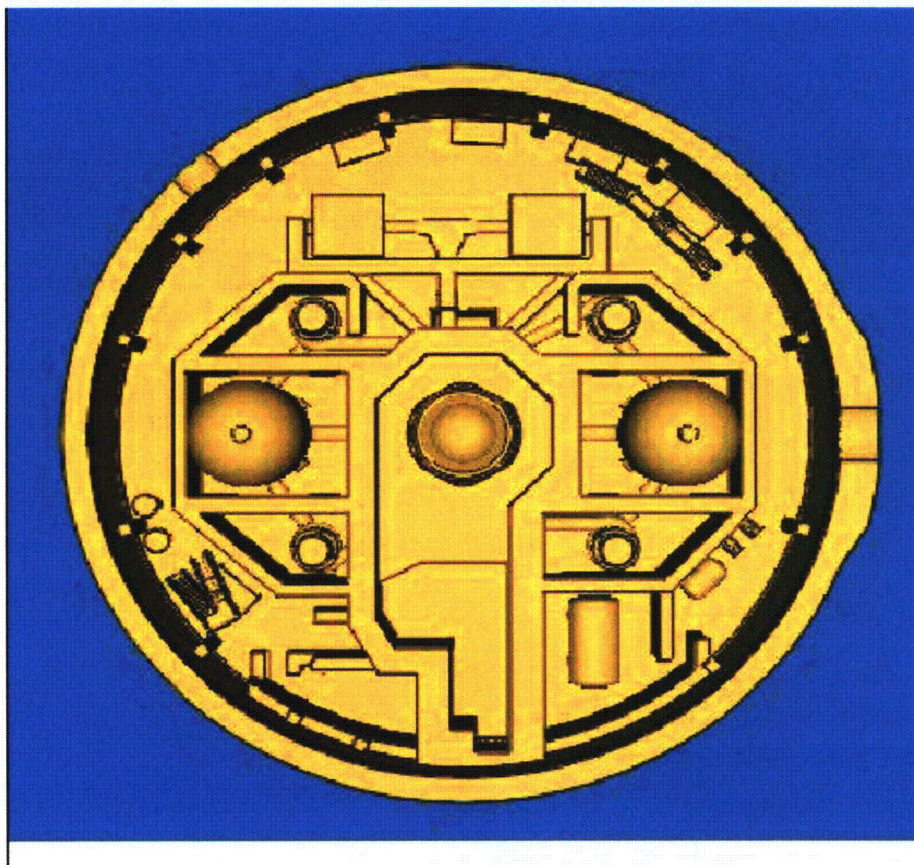


Figure 6
Fort Calhoun Station Containment Geometry

Erosion of Fibrous or Cal-Sil insulation

Erosion of small and large pieces of fibrous insulation is accounted for. Erosion of fibrous insulation is assumed to be at 10% of small and large pieces of fibrous debris and that erosion of debris is transported directly as fines to the strainer without further credit of sedimentation or settling. ~~A 10% erosion fraction was proposed to the NRC during the pilot plant audit process and was considered appropriate.~~ Erosion of small pieces of Cal-Sil insulation is accounted for. Erosion of Cal-Sil insulation was based on actual hydraulic lab testing (Reference 20) and was predicted to be conservatively bounded at 15%. Thus, small pieces of Cal-Sil will be subjected to an erosion fraction of 15% as fines to the strainer without further credit of sedimentation or settling. This is considered conservative as with the significantly low flow pool condition, some of these eroded fibers and Cal-Sil fines could settle out before reaching the strainer.

CFD Analysis and Transport during Recirculation

The CFD calculations for recirculation flow in the FCS containment pool were performed using Flow-3D[®] Version 9.0 with an Alion modified subroutine. The following general steps were taken in modeling the debris transport during the recirculation phase after a postulated LOCA at FCS:

1. Based on the containment building drawings, a three-dimensional (3-D) geometric model of the containment floor was built using CAD software.
2. A computational mesh was generated that sufficiently resolved the key features of the CAD model, but maintained a cell count low enough for the simulation to run in a reasonable amount of time.
3. The dimensions of the solid objects resolved in the computational mesh were checked with the appropriate drawings to verify the accuracy of the model.
4. The boundary conditions used in the CFD model were set based on the operation of FCS during the recirculation phase.
5. At the determined LOCA break location, a mass source was added to account for introduction of the break flow.
6. A negative mass source (mass sink) was added at the sump screen location with a total flow rate equal to the recirculated break flow exiting the postulated ruptured pipe.
7. Appropriate turbulence modeling was enabled.
8. After running the CFD calculation, the kinetic energy averaged across the pool was checked to verify that it was no longer changing significantly, indicating that the case had run long enough to reach steady-state flow conditions.
9. Transport metrics were determined based on relevant tests and calculations for each significant debris type present in the FCS containment building were performed.
10. A graphical determination of the transport fraction of each type of debris was made using the velocity and TKE profiles from the CFD calculation.

With no spray flow, the low sump flow results in pool regions with very low velocity (see Figure 7 below) and respective TKEs (see Figure 8 below). Using the standard methodology, no transport of macro debris including RMI, LDFG, Temp-Mat[®] and paint

uncertainty for the low velocity case, the standard methodology was adjusted to estimate the fine debris transport. It was assumed no transport of fine debris occurred in pool regions with predicted velocities less than the predicted velocities of 0.01 ft/s. The capabilities of Flow-3D® predicting the velocities greater than 0.01 ft/s were validated in a low velocity test carried out in ALION's transparent flume.

The justification of this assumption is as follows:

- Based on the corresponding settling velocities and required TKEs, all fine debris originally were assumed to transport under normal recirculation conditions that have spray flow.
- The transport metric based on very low velocities found in no-spray flow cases results in low transport of fine debris (see Figure 8 below). The pool region showing the iso-surface of required TKE to suspend individual fibers is shown in Figure 8 below, which indicates very low transport or high settling of the individual fibers.
- Based on the truncation error in finite difference equations (FDEs) and the round off error by the computer, the lowest velocities with significance in CFD prediction are expected to be greater than 10^{-4} ft/s.
- Concerns expressed by OPPD and the NRC for this condition led to related experimental work to validate CFD predictions for low velocity conditions. It was shown that FLOW-3D® is capable of predicting low velocities greater than 0.01 ft/s (Reference 21) (See Figure 9 below). **Low flow testing was performed in the ALION transport flume to validate Flow-3D's capabilities of predicting low velocities. Flow measurements were conducted for two flow rates: 16.99 and 32.14 gpm. These flow rates result in an average velocity of 0.012 and 0.024 ft/s through the cross-section of the flume, respectively. These average velocities have the same magnitude as the characteristic velocity in the containment pool for no spray conditions. These low flow conditions in the transport flume were also simulated using Flow-3D®. Comparison between measured velocities in the transport flume and predicted velocities using Flow-3D® confirmed the CFD's ability to accurately predict low flow conditions.** It takes low velocities and turbulent kinetic energy to transport fine debris. These validated CFD predicted velocities are sufficiently large to transport fine debris.
- The characteristic velocity in the flow region of the containment pool has the magnitude of 0.01 ft/s (see Figure 9 below). The stagnant regions are separated from the sump by the regions where the velocities are less than 0.01 ft/s.

Therefore, it was assumed that no transport of fine debris occurs in pool regions with **where predicted velocities are less than 0.01 ft/s and the TKE does not predict high enough turbulence. These regions are considered stagnant regions. Looking at massless particle releases from a break in SG A or B was used along with evaluating the pool velocity 1 inch above the containment floor. (Figure 7) These areas for potential transport were then compared to areas that had sufficient TKE to suspend individual fibers. (Figure 8) Thus, if an area had predicted pool velocity greater than 0.01 ft/sec (which is greater than the settling velocity of most fines) and the TKE was high enough to have suspension (shown in Figure 8 as continuous iso-surfaces), then that area was considered as a fines debris transport area. These regions are considered stagnant regions.** The flow regions identified in Figure 9 are substantially larger than the continuous yellow iso-surface regions shown in Figure 8. Therefore, this assumption is conservative.

Unqualified Coatings

The majority of unqualified coatings in the FCS containment are located at elevations well above the basement floor at elevation 994'. These coatings, should they fail post-DBA, would fail near the component they were applied to and as such, would fall to the concrete slab floor immediately below that component. As can be seen in Figures 10 and 11 below, the FCS containment is comprised predominantly of concrete slab floors at the upper elevations. Thus, if coatings failed they would most likely reside on the component or near it and not fall through gratings. Also, since FCS will not employ containment spray post-LOCA, there will be no motive force (other than condensation washdown) for sliding or driving failed coatings to subsequent lower elevations. Without spray washdown, there would be no water sheeting action to move coatings towards gratings or openings or stairwells and no significant movement of failed unqualified coatings to lower elevations or ultimately to the containment basement floor. Therefore, the failure of unqualified coatings needs only to be evaluated on the containment basement elevation 994'.

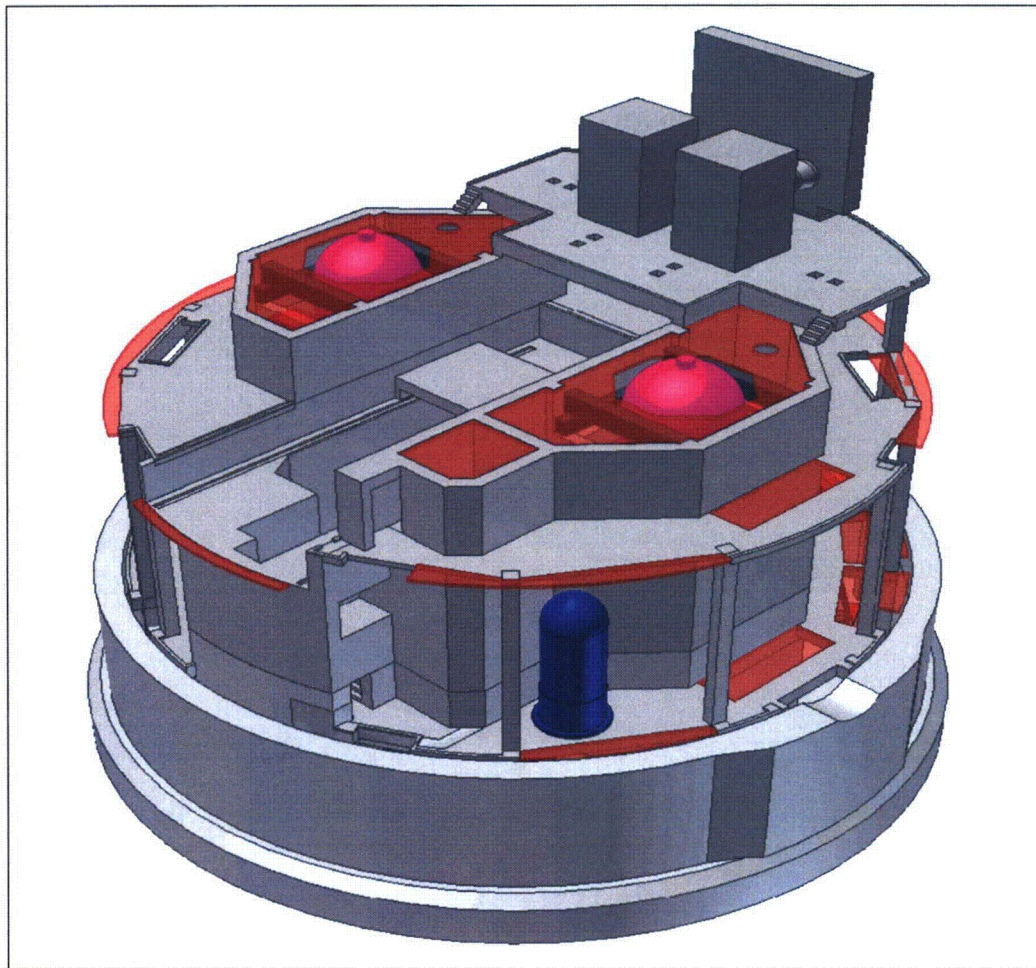


Figure 10
Upper Containment

calculated from the debris generation calculation would be predicted to be at the strainer. The amount of debris in the event of a SBLOCA would then equate to what was calculated from debris generation calculation and shown in Table 17 below.

**Table 17
 SBLOCA results**

Debris Type	Mass or Volume
LDFG (fines)	0.98 ft ³
Cal-Sil (fines)	0.71 ft ³
Unqualified Coatings	22.3 lbm
Qualified Coatings	2 lbm
Particles Latent Debris	40.2 lbm
Fiber Latent Debris	2.2 lbm
Other Latent Debris	37.2 lbm
Stickers, Tape, Labels	71 ft ²
Sand	0 lbm

Table 18 below shows the results of a break at the reactor vessel nozzles, which addresses sand transport.

**Table 18
 RV Nozzle Break Results**

Debris Type	Debris Transport Fraction	Mass or Volume
LDFG (fines)	23%	1.8 ft ³
Stainless Steel RMI	0%	0 ft ²
TempMat [®]	8%	0.9 ft ³
Cal-Sil (fines)	19%	7.8 ft ³
Unqualified Coatings	100%	215.7 lbm
Qualified Coatings	23%	2 lbm
Particles Latent Debris	100% 65%	80.3 52 lbm
Fiber Latent Debris	100% 65%	4.4 3 lbm
Other Latent Debris	100% 65%	74.3 49 lbm
Stickers, Tape, Labels	100%	71 ft ²
Sand (A or B nozzle break)	Varies by break*	121 lbm A side 710 lbm B side

*A break in a penetration that is adjacent to the A SG bay results in sand debris that is blown into the A SG bay, and then subject to transport to the sump strainer. A break in a penetration that is adjacent to the B SG bay results in sand debris that is blown into the B SG bay, and then subject to transport to the sump strainer. A nozzle break on the B SG bay side results in debris that is blown into the bay area that is closest to the sump strainer.

No credit was taken for any debris interceptors at FCS, as they are not installed in containment. Hence, the tables provided above identify the total quantities of each type of debris transported to the strainers for the breaks analyzed.

conclusion that there was a large margin to vortex formation and air ingestion despite the use of conservative assumptions regarding the approach velocity at the strainer surface.

Prototypical Head Loss Testing for the Strainer

Prototypical head loss testing was conducted using module testing (Reference 26). A module test is a head loss test that uses multiple disk sets to simulate a full size strainer. The debris load and flow rate are scaled to simulate plant conditions.

The test module used for all tests except the LBLOCA chemical precipitant test, consists of 15 strainer plates, which are of the same length and width as the plant strainer plate, which is 48" by 33". A sketch of the test module is shown in Figure 13 below. All of the dimensions of the strainer plates including the perforated plate, wire cloth dimensions and internal framework are the same for the test article as they are for the plant strainer. Any differences between the test and plant strainer are noted below:

- For the test module, the outer surface of the disks at each end of the test module are solid sheet material and not perforated plate/wire cloth. These outer test disk frames are half as thickness (1/4") as the inner test disk frame in order to model the flow in the frame cavity that represents flow approaching only from the inner surface of each disk. The test module is mounted on a frame, which is prototypical of the plant configuration.
- The perforated plate thickness for the test module is 0.046" compared with the plant perforated plate thickness of 0.059". This thinner perforated plate was evaluated and shown to be acceptable to handle the expected test conditions without structural damage. This difference has no effect on hydraulic performance.
- The inner cavity diameter is the same for both the test article and plant strainer. The resulting clean head loss from the test article inner cavity will be less than the plant strainer inner cavity clean head loss due to the reduced flow rate and reduced length of the inner cavity in the test. For the clean head loss evaluation, the measured clean head loss from the test is assumed to be due to only the strainer disks and ignores the contribution from the inner cavity. The head loss for the inner cavity is calculated and added to the measured clean head loss to determine a conservative clean head loss for the strainer.

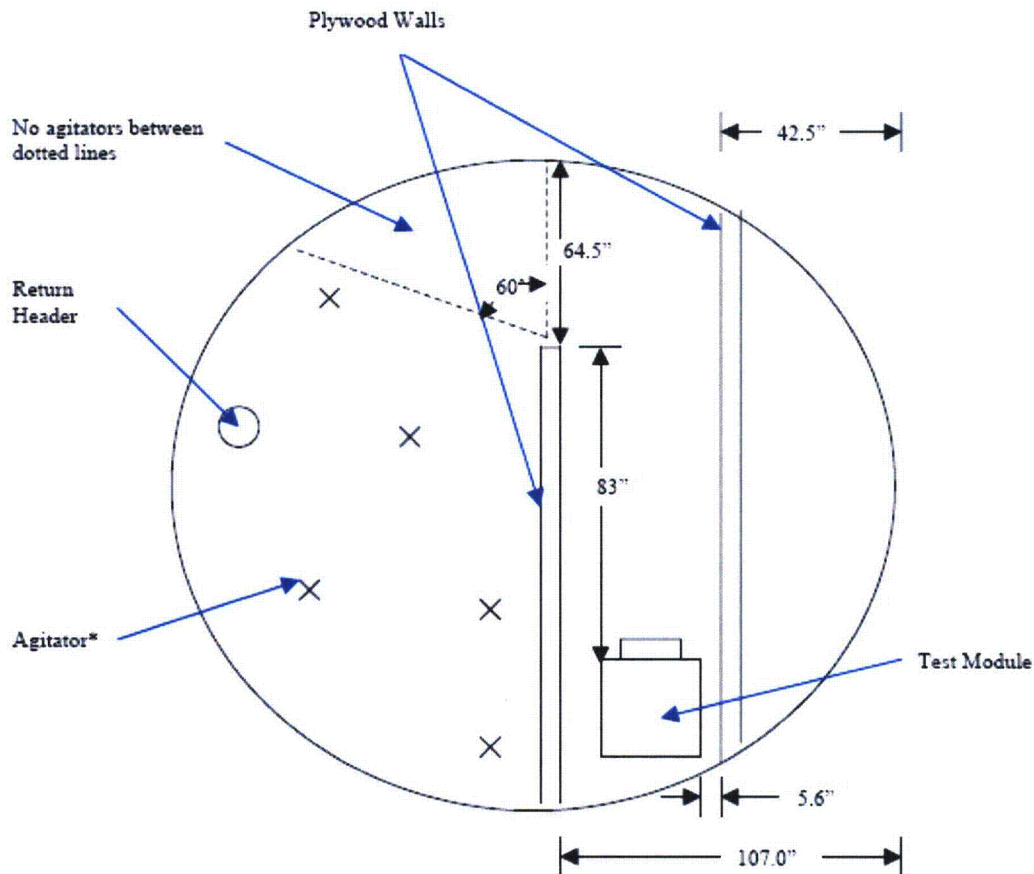


Figure 15
Module Test Configuration (Plan View)

For the SBLOCA, a different test setup was used from the LBLOCA. The small line break location at FCS is located such that the debris transport for Strainer "B" will be bounded by the LBLOCA transport to Strainer "A^B". The LBLOCA test configuration is conservative for the SBLOCA configuration for Strainer "B" and the LBLOCA debris loads bound the SBLOCA. Therefore, the test results for the LBLOCA which models Strainer "B" will bound the SBLOCA for that strainer.

For Strainer "A" there will be a direct path between the break location and the strainer. Consequently, testing for this strainer did not credit near field settling and was well mixed in front of the strainer. Figure 16 below is a plan view of the test setup for the SBLOCA break scenario.

**Table 19
Strainer Head Loss Testing**

Test	Strainer Head Loss (Reference 38) (1)	Maximum Acceptable Head Loss (Reference 37)
LB-LOCA Maximum Debris	0.99 ft (unverified)	5.34 ft
LB-LOCA 0.25" thin bed	2.19 ft (unverified)	5.34 ft
LB-LOCA 0.125" thin bed	2.44 ft (unverified)	5.34 ft
LB-LOCA 0.0625" thin bed	1.71 ft (unverified)	5.34 ft
LBLOCA 0.125" thin bed with Chemical Precipitants	4.41 ft (unverified) (not scaled for temperature)	5.34 ft
SBLOCA with chemical precipitants	3.38 ft (unverified) (Partially scaled for temperature)	4.79 ft

Notes:

- 1) Includes debris and clean head loss
- 2) The SBLOCA "not scaled for temperature" test head loss of 5.88 ft (70.6 inches). This value was partially scaled to the plant head loss shown in the table by employing the methodology provided in the following section.

**Table 19
Strainer Head Loss Testing¹**

Test Label	Clean Head Loss (in)	Flow Rate at Max Head Loss (gpm)	Maximum Head Loss (in)	Temperature at Max Head Loss (°F)
1M-LBLOCA	0.7	499.4	10.9	94.1
2M-LBLOCA -0.25	0.7	497.2	24.9	96.4
3M-LBLOCA -0.125	0.6	495.7	27.5	97.2
4M-LBLOCA -0.0625	0.6	493.7	19.0	93.4
5M-LBLOCA -FCE (0.125)	0.1	176.8	37.9	96.7
6M-RPT	0.1	261.5	49.6	92.2
7M-RPT	0.2	261.0	0.5	96.1
8M-RPT	0.2	261.3	43.4	96.5
9M-RPT	0.1	263.8	32.8	93.5
10M-SBLOCA -LDFG	0.2	257.9	76.2	94.7
11M-SBLOCA -Jacketed	0.2	258.1	70.0	92.5

¹ Note: Results in Table 19 are not scaled or corrected for instrument inaccuracies.

Table 19a - Plant Head Loss Summary

	Scaled Strainer Head Loss (ft)	Clean Head Loss (ft)	Total Head Loss (ft)	Allowable Head Loss Limit (ft)	Head Loss Margin (ft)
5M-LBLOCA -FCE (0.125)	3.357	0.073	3.430	5.34	1.91
11M-SBLOCA -Jacketed	3.243	0.072	3.315	4.79	1.48

Four (4) LBLOCA tests were performed, with thin bed debris loads and without chemical precipitants, to determine the worst debris load case for head loss. The thin bed debris loads consisted of 0.5, 0.25, 0.125 and 0.0625 inches. The results showed the 0.125 inch thin bed resulted in the worst case for head loss. Based on these results, the 5M-LBLOCA incorporated the 0.125-inch thin bed debris load from the 3M-LBLOCA-0.125 together with chemical precipitants to obtain the maximum head loss. (5M-LBLOCA-FCE)

For LBLOCA assuming turbulent flow due to bore holes, the plant head loss is proportional to the square of the ratio of the plant debris bed velocity and test debris bed velocity. (A bore hole is the sudden collapse of the debris bed in a localized area, which allows the turbulent flow of water to pass through the debris bed and strainer perforated plate, resulting in reduced head loss.)

The assumption of turbulent flow is conservative as it precludes scaling by kinematic viscosity, which would yield a significantly reduced head loss compared to laminar flow. The strainer head loss at post LBLOCA recirculation conditions was calculated from the testing head loss results using the following scaling equation:

$$\text{Headloss}_{\text{Debris}} = (\text{HeadLoss}_{\text{Test}} - \text{HeadLoss}_{\text{Test.Clean}}) \cdot (\text{Velocity}_{\text{Plant}} / \text{Velocity}_{\text{Test}})^2$$

Where:

- HeadlossDebris = Scaled head loss due to the debris**
- HeadLossTest = Measured maximum head loss from the test**
- HeadLoss_{Test.Clean} = Measured clean head loss from the test**
- Velocity_{Plant} = Plant approach velocity**
- Velocity_{Test} = Test approach velocity**

$$h_{\text{plant}} = h_{\text{test}} \cdot (V_{\text{plant}} / V_{\text{test}})^2$$

Where:

- h_{plant} = Plant head loss**
- h_{test} = Test head loss**
- V_{plant} = Plant velocity rate per unit area of strainer**
- V_{test} = Test velocity per unit area of test article**

Assuming laminar flow, plant debris head loss is calculated based on the test head loss and the differences between plant and test parameters. The parameters are debris bed velocity, viscosity, debris bed thickness and water density. The relationship between plant head loss, test head loss and the difference in plant and test parameters is based on Darcy's law and the resultant equation is shown below in Equation 3.

Equation (3):

$$\text{Headloss}_{\text{Debris}} = (\text{HeadLoss}_{\text{Test}} - \text{HeadLoss}_{\text{Test.Clean}}) \cdot (\text{Viscosity}_{\text{Plant}} / \text{Viscosity}_{\text{Test}}) \cdot (\text{Velocity}_{\text{Plant}} / \text{Velocity}_{\text{Test}}) \cdot (\text{DebrisThickness}_{\text{Plant}} / \text{DebrisThickness}_{\text{Test}}) \cdot (\text{WaterDensity}_{\text{Test}} / \text{WaterDensity}_{\text{Plant}})$$

Where:

- HeadlossDebris = Scaled head loss due to the debris
- HeadLossTest = Measured maximum head loss from the test
- HeadLossTest.Clean = Measured clean head loss from the test
- ViscosityPlant = Plant water dynamic viscosity at 196.6°F
- ViscosityTest = Test water dynamic viscosity at 94.5°F
- VelocityPlant = Plant approach velocity
- VelocityTest = Test approach velocity
- DebrisThicknessPlant = Plant fiber debris bed thickness
- DebrisThicknessTest = Test fiber debris bed thickness
- WaterDensityPlant = Plant water density at 196.6°F
- WaterDensityTest = Plant water density at 94.5°F

$$h_{l_{\text{plant}}} = h_{l_{\text{test}}} \cdot (v_{\text{plant}} / v_{\text{test}}) \cdot (V_{\text{plant}} / V_{\text{test}}) \cdot (\Delta x_{\text{plant}} / \Delta x_{\text{test}}) \cdot (\rho_{\text{test}} / \rho_{\text{plant}}) \quad \text{Equation 3}$$

Where:

- $h_{l_{\text{plant}}}$ = Plant head loss
- $h_{l_{\text{test}}}$ = Test head loss
- v_{plant} = Plant viscosity of water at RAS 196.6°F
- v_{test} = Test viscosity of water at 95°F
- V_{plant} = Plant flow rate per unit area of strainer
- V_{test} = Test flow rate per unit area of test article
- Δx_{plant} = Plant debris bed thickness
- Δx_{test} = Test debris bed thickness
- ρ_{test} = Test density of water at 95 °F
- ρ_{plant} = Plant density of water at 196.6 °F

During testing for SBLOCA it was evident that bore holes were present in the debris bed. Bore holes cause turbulent flow and will prevent scaling using Equation 3, if there are a significant number of bore holes. If only laminar flow was present, Equation 3 would scale the maximum **repeatability** test-head loss (HL) of 70.6 **68.74** inches, at 400 **92.5**°F to the theoretical plant head loss at 196.6°F and arrive at the laminar flow head loss of 34.04 **33.92** inches. To determine the effect of the bore hole on scaling, the **11M-SBLOCA** test was run, at approximately 400 **92.5**°F, until achieving a maximum head loss of 70.6 inches (corrected for instrumentation accuracy). At this point, the

temperature was reduced to 70 69.7°F and the head loss was allowed to reach a maximum measured head loss of 78.3 inches (corrected for instrumentation accuracy). If the flow had been entirely turbulent the head loss at 400 69.7°F would have remained approximately the same as the head loss at 70 92.5°F. Since the head loss did increase, the flow must be a combination of laminar and turbulent flow and would allow for partial scaling, using Equation 3-above 4. To determine the scaling adjustment factor, Equation 3 is used to scale the maximum head loss at 400 92.5°F (70.6 inches) to the theoretical laminar flow head loss at 70 69.7°F of 91.48 89.82 inches. The scaling adjustment factor is equal to the ratio of the theoretical laminar flow head loss at 70 69.7°F (91.48 89.82 inches) to the maximum measured head loss at 70 69.7°F (78.3 inches). The adjustment factor is then applied to the laminar flow head loss at 196.6°F (34.0 33.92 inches).

~~Plant partially scaled HL at 196.6°F = Adjust Factor x Plant laminar flow HL at 196.6°F~~

~~Adjust Factor = Test laminar flow HL at 70°F / Test maximum measured HL at 70°F~~

~~Plant partially scaled HL at 196.6°F = (91.48 in/78.3 in) x 34.04 in = 39.77 in = 3.31 ft.
 (does not include clean head loss)~~

Where:

~~Plant partially scaled HL at 196.6°F: Plant scaled head loss at 196.6°F using Equation 3 above, adjusted for turbulent flow.~~

~~Plant laminar flow HL: Plant scaled head loss at 196.6°F using Equation 3.~~

~~Test laminar flow HL at 70°F: Test maximum measured head loss at 100°F scaled to head loss at 70°F.~~

~~Test maximum measured HL at 70°F: Test maximum head loss measured at 70°F.~~

~~Repeatability will be included in the head loss evaluation, after the repeatability testing results, based on SBLOCA with chemical precipitants, and incorporated into the deviation analysis.~~

Equation (4):

Plant partially scaled HL at 196.6°F = (Adjust Factor)(Plant laminar flow HL at 196.6°F)

Adjust Factor = $\frac{\text{Test theoretical laminar flow HL at 70°F}}{\text{Test maximum measured HL at 70°F}}$

Plant partially scaled HL at 196.6°F = $\frac{89.82 \text{ in}}{78.3 \text{ in}} \times 33.92 \text{ in}$

= 38.92 in = 3.243 ft (does not include clean head loss)

Where:

Plant partially scaled HL at 196.6°F: Plant scaled repeatability head loss at 196.6°F using EQ (3), adjusted for turbulent flow.

Plant laminar flow HL at 196.6°F: Plant scaled repeatability head loss at 196.6°F using EQ (3).

Test theoretical laminar flow HL at 69.7°F: Test maximum measured head loss at 92.5°F scaled to head loss at 69.7°F.

Test maximum measured HL at 69.7°F: Test maximum head loss measured at 69.7°F

Maximum Volume of Debris Predicted to Arrive at the Screen

The large break LOCA test discussed in the previous section used a scaled debris load based on the maximum amount of debris transported to the strainer.

Thin Bed Formation

The fiber debris loads for the thin bed test results are based on the amount of fiber to provide a nominal bed thickness on perforated plate of 1/4", 1/8" and 1/16", respectively. The test results demonstrate the ability of the strainer to resist or accommodate the formation of the thin bed.

Basis for the Strainer Design Maximum Head Loss

The basis for the strainer maximum allowable head loss is the lesser of the crush pressure of the strainer or the allowable ECCS head loss. The lesser allowable head loss was determined to be the limiting NPSH margin as determined by different combinations of pumps and plant alignment as discussed in Section 3g below.

Significant Margins and Conservatisms Used in the Head Loss and Vortexing Calculations

The strainer head loss and vortexing were measured using testing. In addition, the possibility of vortex formation at the strainers was evaluated using the conservative assumption of increasing the approach velocity by a factor of 3, to simulate the increased flow rate near the suction end of the strainer. Testing was performed using a conservatively low containment sump water level, calculated for the present operating conditions, which assume a considerable volume of water hold up in the refueling cavity and containment spray headers. The water level will be higher following implementation of LAR-07-04 (Reference 16). In addition, the head loss testing for the LBLOCA was conducted using the flows associated with 2 HPSI pumps operating on one header in conjunction with the largest debris load which corresponds to the opposite header.

Methodology, Assumptions, and Results for the Clean Strainer Head Loss Calculation

The clean head loss evaluation is based on a combination of strainer head loss and piping head loss. The strainer head loss is composed of the head loss through the individual disc sets and the central channel. The disc set head loss is based on the module test clean head loss results, which are scaled by the square of the ratio of flow velocities. The central channel uses the resistance coefficient K of a straight pipe to calculate the head loss. The piping uses the resistance coefficient K for the individual piping components to determine head loss of the routing. The maximum clean strainer assembly head loss is 0.423-073 feet for Strainer SI-12B and 0.0724 feet for Strainer SI-12A.

Flashing

An assessment of FCS sump strainer potential for void formation was conducted and documented. The assessment was performed with the following conservative assumptions which provide additional margin: the worst case total head loss across the strainer, conservative containment pool area, and the maximum flow rate through the strainer. In addition, the submergence of the strainer was assumed to be only from the post-LOCA pool water level to the top of the strainer. This is conservative since the strainer perforated flow plates are below the top of the strainer, at a greater submergence; hence there is a higher hydrostatic head with the consequential smaller void fraction. The calculations indicate that for fluid temperatures equal to or less than 205°F the void fraction downstream of the ECCS strainer is less than 3% (at 205°F, the void fraction was estimated to be 2.62%, with no credit for containment overpressure). For the maximum calculated fluid temperature of 213°F, a containment overpressure of 5.4 ft water is required to keep the void fraction less than 3%. Long-term sump temperature and containment pressure analyses for various alignments show that only one case results in sump temperatures above 200°F, for a period of time no longer than 4 hours. The ~ 5 ft. overpressure credit to ensure that the void fraction remains below 3%, is consistent with the overpressure required to ensure adequate net positive suction head (NPSH) available for the high pressure safety injection (HPSI) pumps, as described in Reference 16. The credited overpressure is considerably lower than the available overpressure during that time period, which is well above 20 ft. ~~Flashing is not anticipated to occur since 8.99 feet of containment overpressure is allowable for credit, and the limiting debris loaded strainer head loss is 5.34 feet (References 37 and 39). However, the flashing evaluation cannot be finalized until LAR-07-04 (Reference 16) is approved to allow the licensing basis to credit containment overpressure as alluded to in the NRC RAI (Reference 51).~~

System response is determined by break size and resulting RCS and containment pressure characteristics. The ECCS original design was such that for a large break LOCA, all safety injection and containment spray pumps were started. Amendment 244 (Reference 57) implemented in November 2006 allowed the disabling of the auto-start feature of one CS pump. In 2004, emergency operating and abnormal operating procedures were revised to secure one HPSI pump prior to or shortly following RAS if all three HPSI pumps are in operation (Reference 56).

LAR-07-04 (Reference 16) was submitted by OPPD in July 2007 and is presently under review by the NRC. LAR-07-04 changes the containment spray actuation logic such that the CS pumps will not start during a LOCA. The new CS system actuation logic will require that both the steam generator low signal (SGLS) and the containment spray actuation signal (CSAS) be initiated before the CS system is actuated. Thus, containment spray will not initiate in response to a LOCA, and for a large-break LOCA, only the HPSI and LPSI pumps will inject water into the core. Upon depletion of water in the SIRWT, and initiation of recirculation, the LPSI pumps are automatically stopped and the HPSI pumps are aligned to take suction from the containment sump.

The basis for the containment spray actuation logic change is to improve the NPSH margin for the HPSI pumps by reducing the head loss and hydraulic resistance through the containment sump strainers when the HPSI pumps are operating in the recirculation mode. (The LPSI pumps are automatically shut off following a RAS.) The enhancement in the NPSH performance will be due to reduced transport of debris to the strainer resulting in a reduction in the pressure drop across the strainer and a reduction in piping head loss. This will provide additional margin for the NPSH available ($NPSH_A$) for the HPSI pumps taking suction from the containment sump, increase the amount of water delivered to the core during the injection phase of a LOCA and will increase the time to the initiation of a RAS.

The maximum flow for Train A (Strainer SI-12B) would be 923 GPM and for Train B (Strainer SI-12A) 479 GPM. The flows are based on the calculations of the system performance during the recirculation phase. The worst-case failure from a flow and NPSH margin standpoint is a failure of a LPSI pump to stop at RAS. This failure would result in minimum NPSH margin and maximum flow through one strainer until such time that the pump could be manually stopped by the operators (approximately 10-15 minutes). Additional CFD evaluations for such a condition have shown that this failure would result (under the worst case condition) in loss of only one strainer train. The remaining train would not be affected and will perform its design function. Therefore, no additional NPSH calculations were performed for this case.

The limiting SBLOCA case for debris transport, is a 3" pressurizer spray line in the vicinity of the strainers, because it provides a direct path to the strainers. The debris produced (by the only other line break that can provide a direct path to the strainer) (the 4" Pressurizer Code Safety and PORV lines) is bounded by the LBLOCA debris, as

discussed in section 3b. The NPSH margin for the SBLOCA is not limiting because the pump is injecting against a higher RCS pressure and the NPSH required is lower.

NPSH calculations were performed to establish the ECCS and CS pump NPSH margins in the absence of collected debris (i.e., pump NPSH margins were calculated by subtracting the NPSH required, including the head loss across a clean strainer from the NPSH available.) The required NPSH was taken from the curves provided by the pump manufacturer. The NPSH margin in each case was calculated using a sump temperature of 194.7°F, which corresponds to an equivalent 8.99 feet of subcooling, as credited in the USAR. OPPD has previously requested and received NRC approval for crediting up to and including 8.99 feet of containment overpressure to ensure that NPSH requirements of the pumps are satisfied under the most conservative conditions (i.e. possible pump run-out during a LBLOCA) (Reference 39).

The results shown in the Table 20 below represent the NPSH margin calculated after implementation of the proposed containment spray actuation logic change, when only the HPSI pumps (SI-2A, SI-2B and/or SI-2C) are taking suction from the containment sump.

**Table 20
 Strainer, NPSH and Water Level Margins**

Pump	Case	Strainer	Strainer Flow (gpm)	Minimum NPSH margin (ft)	Containment Water level (ft)*
SI-2A	Train A	SI-12B	479	6.06	3.96
SI-2B	Train B	SI-12A	479	5.34	3.96
SI-2C	Train A	SI-12B	479	5.45	3.96
SI-2A	Train A	SI-12B	923	8.30	3.96
SI-2C	Train A	SI-12B	923	7.74	3.96
SI-2B	Train B	SI-12A	471	6.14	3.41

*Note all water levels are based upon the previous spray configuration, which had water holdup in the refueling cavity, containment spray piping, droplets in the air. As such, in the no-spray configuration the containment water level will actually be higher as there will be no holdup in the refueling cavity or in the piping/containment atmosphere.

NPSH calculations were performed using hydraulic models of the system aligned for ECCS sump recirculation per plant procedures. (Reference 37) Different configurations were modeled and the system configuration resulting in the highest flows was used for testing the installed strainers. The configuration resulting in the smallest NPSH margin was used to determine acceptable screen head loss. The calculations use the Proto-Flow model developed to represent the safety injection piping at FCS. The calculations used the FLO-SERIES Pipeline Reports to determine the head loss in the piping system. Fixed hydraulic resistances (K values) provided for specific valves (when available) were used to calculate the flow coefficient (C_v) values and head loss through the components.

Sump temperature post-RAS was determined as part of the analyses performed to evaluate the containment response without containment spray system initiation.

The water inventory required to ensure adequate sump pool level and sump pool flow paths was evaluated. The containment water level calculation was developed following walkdowns performed during the 2003 and 2005 RFOs that identified water holdup volumes in the refueling cavity and around the reactor vessel ~~were identified~~. Flow past the **Reactor Pressure Vessel (RPV)** flange seal is credited as an alternate flow path. This condition was found acceptable for the current design, however, to minimize water holdup and increase sump pool depth (for increased NPSH margin), a modification to install spacers in the RPV flange was implemented during the 2006 RFO (Reference18). The water holdup due to the 4-inch diameter drain line in the refueling cavity will no longer be applicable after implementation of LAR-07-04 since the most significant source of water in the refueling cavity was the containment spray water. Installed and planned modifications to plant systems minimized water hold-up, however submergence and available NPSH were calculated using previous configuration and will be conservative following implementation of the water management initiative.

The inputs into the water level calculation are extremely biased toward minimizing the containment water level. The volumes of the tanks contributing to the sump level calculation were assumed to be at their **Technical Specifications (TS)** minimum required volume, with maximum instrument measurement uncertainty. This is conservative because it results in the minimum volume injected for all water sources into the containment post-LOCA and results in minimum water level in containment. Minimum sump volume is conservative for evaluating submergence of the strainer and therefore potential for vortexing and flashing. It is also conservative for calculating the available NPSH for the pumps taking suction from the sump

The charging pumps would normally operate but no credit is taken for charging pump operation and thus boric acid storage tank (BAST) volume during any LOCA analysis. Therefore, as conservatism, the BASTs were not considered as a source in the water level calculation. (The inclusion of the BAST volume would add approximately 0.3" to the sump pool.) Following installation of the replacement steam generators, RCS volume increased by about 100 ft³, this increase is conservatively omitted from the water level calculation.

The water level calculation (Reference 10) conservatively accounts for the sources of water on the containment floor and for water holdup mechanisms and associated volumes. Determination of the minimum water level accounted for water holdup in the following locations:

- Volume held up as vapor in the containment atmosphere.
- Volume held up on the containment floors above the 994' elevation, including the refueling cavity.
- Volume held up in condensation on heat sink surfaces.
- Volume held up as mist (droplets) in the atmosphere.
- Volume required to fill risers and establish containment spray.

For debris generation and transport analysis, 10 micron particles were assumed for "Acceptable" coatings within the 5D ZOI. "Acceptable" coatings outside the 5D ZOI were not assumed to fail.

All "Indeterminate" and "Unacceptable" (Reference 55) coatings are considered to fail. This is consistent with NEI-04-07, which considers all indeterminate and unacceptable coatings as a single category of coating, producing debris of the same characteristics independent of the type of coating when immersed in the post-DBA pool.

~~Testing performed for Comanche Peak Steam Electric Station by Keeler & Long (Reference 11) has been reviewed and found applicable to the degraded DBA-qualified epoxy and inorganic zinc coatings applied at FCS. In the test, epoxy topcoat / inorganic zinc primer coating system chips, taken from the Comanche Peak Unit 1 containment after 15 years of nuclear service, were subjected to DBA testing in accordance with ASTM D 3911-03. In addition to the standard test protocol contained in ASTM D 3911-03, 10 μm filters were installed in the autoclave recirculation piping to capture small, transportable particulate coating debris generated during the test.~~

~~Reference 11 shows that inorganic zinc predominantly fails in a size range from 9 to 89 microns with the majority being between 14 and 40 microns. Therefore, a conservative size of 10 microns was assumed for transport and headloss analysis of inorganic zinc. Reference 11 also shows that DBA-qualified epoxy that has failed as chips by delamination tend to remain chips in a LOCA environment. The data showed that almost all of the chips remained larger than 1/32 inch diameter. Therefore, a chip diameter of 1/32 inch may be used for transport for Phenoline 305 epoxy coatings shown to fail as chips by delamination. Carboline Phenoline 305, according to manufacturer's product data sheets and material safety data sheets (MSDSs), is conservatively representative of the other DBA-qualified/Acceptable epoxy coatings found in U.S. nuclear power plants, including Mobil 78, Mobil 89, Amercoat 66, Keeler & Long 6548/7107 and Keeler & Long D-1 and E-1 (Reference 12).~~

~~For original equipment manufacturer (OEM) coatings, the Reference 13 EPRI Report "Design Basis Accident Testing of Pressurized Water Reactor Unqualified Original Equipment Manufacturer Coatings," was used to determine that 10 microns is a very conservative assumption for particle sizes. None of the OEM coatings failed as chips. This report also showed that, on average, much less than half of OEM coatings detached and failed during testing. Based on the EPRI test results and the conservative assumption of 10 micron particle size, 100% failure of all OEM coatings is overly conservative.~~

Based on the review of Reference 13 unqualified coatings, OPPD could not reduce the failure percentage across the board for all non qualified OEM coatings. However, based on the review of the EPRI report and plant specific coating types, a reduction in the failure percentage for the Phenoline 305 and Amercoat No. 66 Topcoat could be justified.

3j Screen Modification Package

NRC Guidance

The objective of the screen modification package section is to provide a basic description of the sump screen modification.

- *Provide a description of the major features of the sump screen design modification.*
- *Provide a list of any modifications, such as reroute of piping and other components, relocation of supports, addition of whip restraints and missile shields, etc., necessitated by the sump strainer modifications.*

OPPD Response

The scope of the modification was to perform the hardware changes required to bring FCS into full resolution with GSI-191. This modification, installed during the 2006 RFO, replaced the existing screens for the plant located outside the shield walls on the basement floor of the containment.

The horizontal stacked disk strainers (Figures 18 and 19 below) for FCS Trains A and B consist of a series of 30 horizontally stacked square disks, which are 48" x 33" x 1.22" thick with a 20" O.D. disk spacer in the center. These disks consist of a 1/2" inch frame or internal structure with one perforated plate on each side, 0.059" thick, with 1/16" holes on 7/64" staggered centers with approximately 30% open area and one wire cloth on each side with 0.120" wire diameter, 0.38" opening size and approximately 58% open area. The disks are installed with a 3.0" pitch, which includes a 1.76" nominal gap between adjacent wire cloths. **The perforated plate approach velocity is conservatively calculated to be 0.0052 ft/sec for the LBLOCA and 0.0030 ft/sec for the SBLOCA.** ~~is will reduce approach velocity to the screens to 0.004 fps.~~ The strainer configuration is designed to withstand the allowable head loss to 5.3 feet during post-LOCA design conditions.

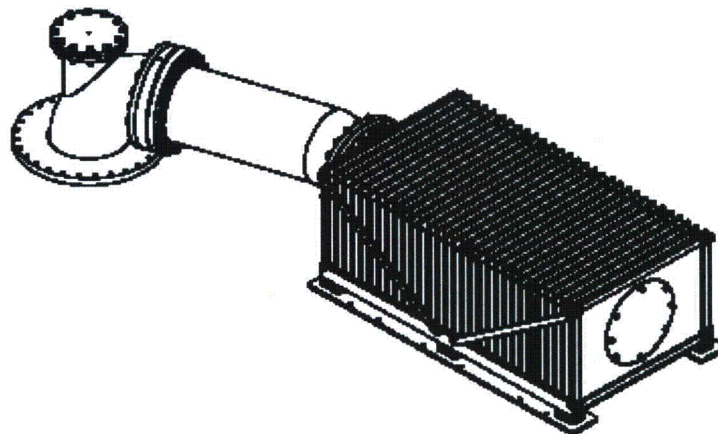


Figure 18
FCS Single Strainer Module

minimum stress ratios are shown in Table 23 and Table 24 below based on the minimum properties and minimum stress allowable. The analysis results show that the ASME code requirements are satisfied for all of the structural components and welds.

Table 23
Stress Ratio Summary for Strainer Components
based on ASME Code Subsection NC

Component	Service Level	Stress Ratio*
Perforated Plates	Design	3.91
Fingers	Design	7.86
Frame and End Cap	Design	13.46
Spacers	Design	7.39
Base	Design	5.10
Outer Rods	Design	3.26
Inner Rods	Design	3.71
Pipe	Design	27.32
Perforated Plates	Level – B	4.30
Fingers	Level – B	8.64
Frame and End Cap	Level – B	14.81
Spacers	Level – B	8.13
Base	Level – B	5.61
Outer Rods	Level – B	3.59
Inner Rods	Level – B	4.08
Pipe	Level – B	30.06
Perforated Plates	Level – D	6.26
Fingers	Level – D	12.57
Frame and End Cap	Level – D	21.53
Spacers	Level – D	11.82
Base	Level – D	8.16
Outer Rods	Level – D	5.22
Inner Rods	Level – D	5.93
Pipe	Level – D	43.71

*Stress Ratio = ASME Stress Limit/Calculated Max. Stress

Table 24
Stress Summary for Welds based on Service level D Load

Weld Location	Weld Stress (psi)	Allowable Stress** (psi)	Stress Ratio*
Perforated Plate to Finger	4,681.42	8,164	1.74
Perforated Plate to Frame	9,272.50	9,342	1.01

*Stress Ratio = ASME Code Stress Limit/Calculated Stress

**Conservative Level A Stress Limits, ASME Code Section III, Subsection ND-3923 at 188 °F

The load due to differential pressure for the sump strainer was determined to be able to withstand a crush pressure of 7 psi (Reference 43).

The test results show that a total of 24.135 gr (grams) of dry fiber bypassed the strainer out of a total of 5084.74 gr (or 0.47%). The total plant strainer fiber bypass was then calculated based on testing results and applying linear scaling of the measured tested fiber bypass. The total bypass consists of the measured fiber bypass plus an additional amount associated with linear extrapolation of the bypass rate at test termination over a 30 day period. This is shown as follows:

Bypass test = Bypass measured + Bypass 30 day

Bypass rate was determined to be 0.12 gr dry fiber in 60 minutes based on measured data.

Therefore,

Bypass 30 day = $(0.12\text{g}/60\text{ min}) \cdot (30\text{ days}) \cdot (24\text{ hours}/\text{day}) \cdot (60\text{ min}/\text{hr})$

Bypass 30 day = 86.40 gr

Bypass measured = 24.135 gr

Bypass test = $24.135\text{ gr} + 86.40\text{ gr} = 110.535\text{ gr}$

This amount of fiber is a small fraction of the initial loading on the strainer. The total bypass fraction for 30 days is therefore,

Bypass fraction = $110.535\text{ gr}/5084.74\text{ gr} = 2.2\%$

The amount of debris that could be anticipated to bypass the plant specific strainer is then calculated:

Bypass test = 110.535 gr = 0.2437 lbm

Area of plant strainer = ~~523~~ 516.3 ft²

Aptest = 22.8 ft²

Bypass plant = $(0.2437\text{ gr}) \cdot (516.3/22.8\text{ ft}^2)$

Bypass plant = 5.529 lbm

Based on a micro density of TempMat[®] material of 162 lbm/ft³ the volume of fibers would equate to 0.035 ft³. This is a very small fraction of TempMat[®] material considering the initial load. The actual volume of fibrous debris is quite low in comparison to the amount of debris that was assumed for downstream wear effects (10 ft³). Thus, the actual measured/calculated bypass is approximately a factor of over 200 less than what was evaluated for downstream effects on components, and systems.

The amount of material calculated above was used for determining the chemical effects in the vessel and with fuel using the methodology described in WCAP-16793 (LOCADM calculations) (References 50 and 53). The preliminary calculations indicate with the maximum debris case a fuel clad scale thickness at 37.8 microns (using double the

5. References

1. Calculation FC06985, Revision 1, "Fort Calhoun Station Debris Generation Post-LOCA"
2. Enercon Services Report OPP003-RPT-001 Rev. 1, "Containment Insulation Summary Master 2006 Update"
3. ALION-REP-ALION-2806-01, Revision 3, "Insulation Debris Size Distribution for Use in GSI 191 Resolution"
4. WCAP-16568-P, "Jet Impingement Testing to determine the Zone of Influence (ZOI) for DBA Qualified/Acceptable Coatings, Revision 0, June 2006"
5. Not Used
6. NUREG/CR-6808, "Knowledge Base for the Effect of Debris on Pressurized Water Reactor Emergency Core Cooling Sump Performance," LA UR 03 0880, 2003.
7. LANL Report "Characterization of Latent Debris from Pressurized Water Reactor Containment Buildings", M. Ding et al NEA/NRC Workshop on Debris Impact on Emergency Coolant Recirculation Paper, April 26, 2004.
8. ALION-REP-OPPD-3016-001, Revision 0, "OPPD Calcium Silicate Material Characterization Report (SEM)"
9. ALION-REP-OPPD-3016-002, Revision 0, "Calcium Silicate with Asbestos Material Characterization Report (SEM)"
10. Calculation FC07010, "Calculation of Design Basis Minimum Containment Post-RAS Level"
11. Keeler and Long Report No. 06 0413, "Design Basis Accident Testing Coating Samples from Unit 1 Containment, TXU Comanche Peak SES"
12. Letter from J. Cavallo, Vice President Corrosion Control Consultants and Labs, Inc., dated September 20, 2007
13. EPRI Report No. 1011753, September 2005, for Original Equipment Manufacturers (OEM)
14. Bostelman, Jan and Zigler Gil, "Failed Coatings Debris Characterization, Prepared for BWROG Containment Group Committee, ITS Services, Duke Engineering & Services, ~~July 21,~~ August 26, 1998"
15. EPRI Report No. 1014883, "Plant Support Engineering Adhesion Testing of Nuclear Coating Service Level 1 Coatings," August 2007
16. Letter from OPPD (D. J. Bannister) to NRC (Document Control Desk), "Fort Calhoun Station Unit No. 1 License Amendment Request (LAR) Modification of the Containment Spray System Actuation Logic", dated July 30. 2007 (LIC-07-0052)
17. Calculation FC07431, Revision 1, GE Calculation 26A7104, "Suction Strainers Stress Analysis Report"
18. Modification EC 36443, "Install a 3/8" Spacer Under Reactor Seal Ring"
19. Calculation FC07460, Sargent & Lundy Calculation 2005-10600, "GSI 191 Evaluation of the Long Term Downstream Effects of LOCA Generated Debris"
20. ALION-REP-LAB-2352-101, Revision 0, "Test Report: Flow Erosion Testing of Cal-Sil Insulation Debris"

21. ALION-REP-LAB-2352-107, "Measurement of Localized Low Velocities in Transport Flume Testing Report"
22. Calculation FC07248, "OPPD Chemical Product Generation Report"
23. WCAP-16530, "Evaluation of Post-Accident Chemical Effects in Containment Sump Fluids to Support GSI-191"
24. WCAP-16785-NP, "Evaluation of Additional Inputs to the WCAP-16530-NP Chemical Model," May 2007
25. Calculation FC07090, Sargent & Lundy Calculation 2005-08220, Revision 0
26. GEH Document, 26A7408 Rev. 2, Fort Calhoun, "Module Head Loss Testing of Sump Strainers"
27. GEH Document, Deviation Disposition Request, 437004232-004
28. 6898-631-01, "5M-LBLOCA-FCE-Verified"
29. 6898-715-01, "11M-SBLOCA-Jacketed-Verified"
30. GENE-0000-0039-6317-R12, "Design Input Request (DIR) S0100," Rev. 12
31. 0000-0081-2633-R0, "FCS Strainer Air Ingestion Analysis"
32. 234C9215, Rev 4, "ICD, Passive Strainer, 48x33, 30 Disk"
33. Letter from OPPD (H. J. Faulhaber) to NRC (Document Control Desk) "Revised Request for an Extension to the Completion Date for Corrective Actions Taken in Response to Generic Letter 2004-02," dated June 9, 2006 (LIC-06-0067)
34. Letter from OPPD (H. J. Faulhaber) to NRC (Document Control Desk) "Correction to Revised Request for an Extension to the Completion Date for Corrective Actions Taken in Response to Generic Letter 2004-02," dated June 12, 2006 (LIC-06-0069)
35. Letter from OPPD (H. J. Faulhaber) to NRC (Document Control Desk) "Supplement to Revised Request for an Extension to the Completion Date for Corrective Actions Taken in Response to Generic Letter 2004-02," dated June 28, 2006 (LIC-06-0070)
36. WCAP-16851-P, Revision 0, "Florida Power and Light Jet Impingement Testing of Cal-Sil Insulation," dated October 2007
37. Calculation FC07078, "Recirculation Phase System Performance for Safety Injection and Containment Spray Systems"
38. GE Test Report, S00100, Report # 0000-0075-4537, **Rev. 2**
39. Letter from NRC (L. R. Wharton) to OPPD (S. K. Gambhir) "Fort Calhoun Station, Unit No. 1 – Generic Letter 97-04, Assurance of Sufficient Net Positive Suction Head for Emergency Core Cooling and Containment Heat Removal Pumps" (TAC No. M99992)" dated March 7, 2000 (NRC-00-0031)
40. Letter from NRC (C. Haney) to OPPD (R. T. Ridenoure), "Fort Calhoun Station, Unit No. 1 - Generic Letter 2004-02 Extension Request Approval (TAC No. MD2323)," dated August 14, 2006 (NRC-06-0103)
41. Modification EC37048, "Replacement of Drain Covers"
42. ALION-CAL-OPPD-4089-01, Revision 0, "Fort Calhoun Station Aluminum Walkdown Report"
43. Fort Calhoun Nuclear Station GE-Hitachi "Recirc Sump Strainer Disc Crush Pressure Analysis" (FC07408)

1. Overall Compliance

Fort Calhoun Station (FCS) will be in compliance with the regulatory requirements listed in the Applicable Regulatory Requirements section of Generic Letter (GL) 2004-02 upon completion of the upcoming refueling outage (RFO) currently scheduled for May 24, 2008.

The Applicable Regulatory Requirements section of NRC Generic Letter (GL) 2004-02 states:

NRC regulations in Title 10, of the Code of Federal Regulations Section 50.46, 10 CFR 50.46, require that the ECCS have the capability to provide long term cooling of the reactor core following a LOCA. That is, the ECCS must be able to remove decay heat, so that the core temperature is maintained at an acceptably low value for the extended period of time required by the long lived radioactivity remaining in the core.

Similarly, for PWRs licensed to the General Design Criteria (GDCs) in Appendix A to 10 CFR Part 50, GDC 38 provides requirements for containment heat removal systems, and GDC 41 provides requirements for containment atmosphere cleanup. Many PWR licensees credit a CSS, at least in part, with performing the safety functions to satisfy these requirements, and PWRs that are not licensed to the GDCs may similarly credit a CSS to satisfy licensing basis requirements. In addition, PWR licensees may credit a CSS with reducing the accident source term to meet the limits of 10 CFR Part 100 or 10CFR50.67. GDC 35 is listed in 10CFR50.46(d) and specifies additional ECCS requirements. PWRs that are not licensed to the GDCs typically have similar requirements in their licensing basis.

Exceptions to the applicable regulatory requirements of GL 2004-02 for FCS are as follows:

The Omaha Public Power District (OPPD) License Amendment Request (LAR) 07-04 (Reference 16) was submitted to the NRC for approval of a change in the containment spray system (CSS) actuation logic, which will eliminate automatic containment spray initiation for a loss-of-coolant accident (LOCA). Following NRC approval, FCS will no longer credit the CSS for heat removal capacity or for iodine removal post-LOCA. The CSS will continue to actuate during a main steam line break (MSLB), which does not require use of safety injection pumps in the recirculation mode. Compliance with the regulatory requirements of GL 2004-02 is based on NRC approval of the LAR by April 1, 2008, so that the proposed changes can be implemented during the 2008 RFO.

Compliance will be achieved through analysis, plant specific testing, larger sump strainers installed in 2006, implementation of LAR-07-04 removing containment spray (CS) for containment pressure mitigation during a LOCA as part of water management initiative strategies, completed plant modifications that reduce debris, and associated programmatic and process changes to ensure continued compliance.

will be lower than the available net positive suction head (NPSH) margin. The results of testing demonstrate that the FCS strainer design is capable of operating under both LBLOCA and SBLOCA scenarios without generating a vortex, which would result in the entrainment of air into the strainers and the emergency core cooling system (ECCS).

The revised containment spray configuration will maintain post-LOCA core injection and required flow through the containment sump strainer while minimizing the bulk containment sump pool debris transport.

For NPSH margin calculations refer to detailed assessments provided in Section 3.g.

Programs are in place to control insulation and coatings inside containment. Controls include inspections of containment coatings each RFO and assessment and engineering evaluation prior to changeout or removal of insulation. Configuration control checklists exist (See OPPD response to 3i) that require prior evaluation of any changes to the amount of aluminum in containment.

FCS has undergone extensive containment cleaning programs since 2003 including the major component replacement projects (SG, PZR and RPV head) of the 2006 RFO. Containment closeout and foreign material exclusion programs ensure that debris is monitored or controlled within design limits.

In conclusion, OPPD is taking the appropriate actions in response to GL 2004-02 to ensure acceptable ECCS performance in the recirculation mode. With the completed actions (i.e., new sump strainers, replacement of sump buffering agent, insulation removal), detailed analyses and testing, and implementation of the modification to CSS actuation logic following NRC approval of LAR-07-04, OPPD is in compliance with the requirements of GL 2004-02. Long-term programs for control and monitoring of debris will ensure that the ECCS will continue to conform to the requirements of GL 2004-02.

Remaining actions outlined in this response required to address the issues in GL 2004-02 will be completed by the dates established between OPPD and the NRC. The configuration of the plant that will exist once all 2008 RFO modifications and actions are implemented for regulatory compliance is discussed next.

Filter Media – Charcoal & Fiberglass

NEI 04-07 (Reference 48) has insufficient data or direction regarding the destruction pressures or debris size distribution of generic low-density fiberglass. Absent applicable experimental data, a value of 100% small fines is adopted by this analysis for filter media in a ZOI. Per the walkdown packages, no filter media is located within the bioshield and is therefore not subject to debris generation as a result of a LOCA. All of the charcoal media is located on the operating floor elevation of 1060' and all of the fiberglass media is on the 1060' elevation or outside the bioshield. This filter media is outside of any ZOI and is not subject to direct containment spray impingement; therefore, filter media is not considered a credible debris source.

Pabco® HD Supertemp (Calcium Silicate) Fire Barrier Board Panel

Absent applicable experimental data, a value of 100% small fines is adopted by this analysis for Pabco® HD Supertemp in a ZOI. Per the walkdown packages, no Pabco® HD Supertemp is located within the bioshield and is therefore not subject to debris generation as a result of a LOCA.

Fiberglass – E-glass Installed at Inlet Nozzles of Reactor Vessel

Approximately 150 feet of fiberglass rope have been installed at the inlet nozzles of the reactor vessel to fill gaps in an effort to reduce heat losses. This is the only fibrous debris source in the case of a reactor vessel nozzle break.

Break No. 1 – Largest Potential for Debris

The LBLOCA in the RCS is the controlling break in terms of quantity of debris generated. The quantities of debris source material are distributed in the FCS containment as follows:

**Table 5
 Insulation Quantity by Location**

Insulation Type	Inside Bio-shield	Outside Bio-shield	Total
Asbestos (ft ³)	353.11	358.35	711.46
Calcium Silicate (ft ³)	16.68	33.20	49.88
Cerafiber (ft ³)	2.35	1.93	4.28
Fiberglass (ft ³)	381.86	969.97	1351.83
Foam Rubber (ft ³)	0.97	11.08	12.05
NUKON® (ft ³)	4.73	16.24	20.96
Pabco® HD Supertemp (ft ³)	0.00	12.69	12.69
Phenolic Bonded Glass Fiber (ft ³)	0.00	800.00	800.00
Temp-Mat® (ft ³)	189.90	43.92	233.82
RMI (ft ²)	105483.98	0.00	105483.98

Given the arrangement of the RCPs and steam generators (SGs), a fully offset double-ended guillotine break (DEGB) in the hot leg just prior to the vertical rise would most likely destroy the maximum amount of insulation. A 32-inch break of piping (hot leg)

Table 6
Break No. 1 LBLOCA

Debris Type	Debris Size	Debris Quantity Generated (ft ³)			
		RC-2A Hot Leg SG A Bay	RC-3A Cold Leg SG A Bay	RC-2B Hot Leg SG B Bay	RC-3D Cold Leg SG B Bay
Stainless Steel RMI (ft ²)	Fines (<0.25")	9931.80	9931.80	9931.80	9931.80
	Small Pieces (<4")	19863.60	19863.60	19863.60	19863.60
	Large Pieces (>4")	3310.60	3310.60	3310.60	3310.60
	Total	33106.00	33106.00	33106.00	33106.00
TempMat® (ft ³)	Fines	9.51	7.44	5.38	0.96
	Small Pieces (<6")	37.01	29.55	21.13	3.71
	Large Pieces (>6")	33.16	6.76	13.10	4.40
	Intact Pieces (>6")	35.23	7.18	13.91	4.67
	Total	114.91	50.93	53.52	13.75
LDFG - NUKON® (ft ³)	Fines	0.04	0.02	0.65	0.11
	Small Pieces (<6")	0.18	0.02	2.68	0.09
	Large Pieces (>6")	0.00	0.09	0.57	0.55
	Intact Pieces (>6")	0.00	0.10	0.60	0.59
	Total	0.22	0.22	4.51	1.34
LDFG - Fiberglass (ft ³)	Fines	20.96	11.10	19.16	11.63
	Small Pieces (<6")	70.73	36.08	72.10	39.99
	Large Pieces (>6")	21.77	18.09	8.32	18.55
	Intact Pieces (>6")	23.35	19.37	8.92	19.83
	Total	136.78	84.64	108.50	89.99
Cal-Sil (ft ³)	Particulate	2.48	0.16	0.61	0.03
	Pieces > 1"	2.48	0.11	0.40	0.02
	Total	4.96	0.27	1.01	0.06
Cal-Sil (w/ Asbestos) (ft ³)	Particulate	21.67	8.68	22.91	20.02
	Pieces > 1"	17.46	6.15	15.03	16.73
	Total	39.13	14.83	37.94	36.75
Cerafiber (ft ³)	Total (Fines)	0.63	0.63	1.72	1.72
Foam Rubber (ft ³)	Total (Fines)	0.54	0.54	0.43	0.43
Sand (ft ³)	Total (Fines)	0.00	0.00	0.00	0.00

The quantity of RMI insulation destroyed is very conservative as the destruction pressure for RMI is much higher than that of fibrous insulation and would equate to a much smaller ZOI. However, this conservative result has little impact on sump screen performance compared to the effects of the fibrous insulation, as the transport analysis will show.

Break No. 2 – Large breaks with two or more different types of debris

Break No. 1 has the largest amount of insulation and has several different types of debris. Therefore, the debris generation of Break No. 1 envelopes that of Break No. 2. The intent of Break No. 2 is to ensure that the analysis considers breaks with the potential to transport a variety of debris types. For example, a break with fiber and particulate debris could result in higher head loss across the sump screen than a break with only fiber, even if the latter break produces a much greater quantity of fiber. Since the Break No. 1 cases all generate a variety of debris types (high-density fiber, low-

compartmentalized into two distinct steam generator bay areas. On the right side of Figure 6 is the A SG bay area, and on the left side of Figure 6 is the B SG bay area. The bay areas are not connected to each other at the basement floor elevation, hence water or debris that is generated in one bay area cannot flow or transport directly to the other one. There are two distinct entrances to the bay areas. Each entrance has a key locked chain link fence type door. There are gaps at the bottom of each screened door and on the sides (5" x 38"). In addition, the doors are locked open during power operations, therefore water from the SG bays is not prevented from reaching the sump strainers. The depth of the FCS sump pool is fairly significant (at least 4'). The entrance to the reactor cavity is not inside these bay areas, any water entrained with debris that would get to the reactor cavity shaft would not be held up and would spill over.

Blockage in the refueling canal is not an issue for FCS; with a no-spray configuration there will not be any significant water flow into the refueling canal.

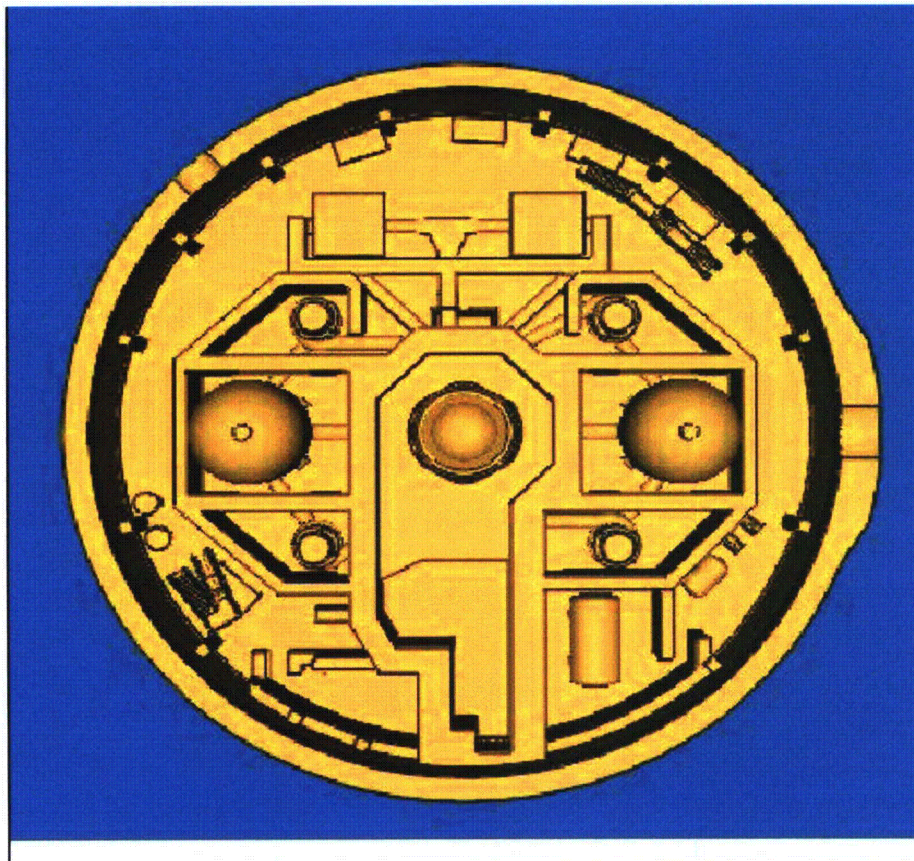


Figure 6
Fort Calhoun Station Containment Geometry

Erosion of Fibrous or Cal-Sil insulation

Erosion of small and large pieces of fibrous insulation is accounted for. Erosion of fibrous insulation is assumed to be at 10% of small and large pieces of fibrous debris and that erosion of debris is transported directly as fines to the strainer without further credit of sedimentation or settling. Erosion of small pieces of Cal-Sil insulation is accounted for. Erosion of Cal-Sil insulation was based on actual hydraulic lab testing (Reference 20) and was predicted to be conservatively bounded at 15%. Thus, small pieces of Cal-Sil will be subjected to an erosion fraction of 15% as fines to the strainer without further credit of sedimentation or settling. This is considered conservative as with the significantly low flow pool condition, some of these eroded fibers and Cal-Sil fines could settle out before reaching the strainer.

CFD Analysis and Transport during Recirculation

The CFD calculations for recirculation flow in the FCS containment pool were performed using Flow-3D[®] Version 9.0 with an Alion modified subroutine. The following general steps were taken in modeling the debris transport during the recirculation phase after a postulated LOCA at FCS:

1. Based on the containment building drawings, a three-dimensional (3-D) geometric model of the containment floor was built using CAD software.
2. A computational mesh was generated that sufficiently resolved the key features of the CAD model, but maintained a cell count low enough for the simulation to run in a reasonable amount of time.
3. The dimensions of the solid objects resolved in the computational mesh were checked with the appropriate drawings to verify the accuracy of the model.
4. The boundary conditions used in the CFD model were set based on the operation of FCS during the recirculation phase.
5. At the determined LOCA break location, a mass source was added to account for introduction of the break flow.
6. A negative mass source (mass sink) was added at the sump screen location with a total flow rate equal to the recirculated break flow exiting the postulated ruptured pipe.
7. Appropriate turbulence modeling was enabled.
8. After running the CFD calculation, the kinetic energy averaged across the pool was checked to verify that it was no longer changing significantly, indicating that the case had run long enough to reach steady-state flow conditions.
9. Transport metrics were determined based on relevant tests and calculations for each significant debris type present in the FCS containment building were performed.
10. A graphical determination of the transport fraction of each type of debris was made using the velocity and TKE profiles from the CFD calculation.

With no spray flow, the low sump flow results in pool regions with very low velocity (see Figure 7 below) and respective TKEs (see Figure 8 below). Using the standard methodology, no transport of macro debris including RMI, LDFG, Temp-Mat[®] and paint

chips and low transport fraction of individual fibers were predicted. To avoid calculation uncertainty for the low velocity case, the standard methodology was adjusted to estimate the fine debris transport. It was assumed no transport of fine debris occurred in pool regions with predicted velocities less than the predicted velocities of 0.01 ft/s. The capabilities of Flow-3D® predicting the velocities greater than 0.01 ft/s were validated in a low velocity test carried out in ALION's transparent flume.

The justification of this assumption is as follows:

- Based on the corresponding settling velocities and required TKEs, all fine debris originally were assumed to transport under normal recirculation conditions that have spray flow.
- The transport metric based on very low velocities found in no-spray flow cases results in low transport of fine debris (see Figure 8 below). The pool region showing the iso-surface of required TKE to suspend individual fibers is shown in Figure 8 below, which indicates very low transport or high settling of the individual fibers.
- Based on the truncation error in finite difference equations (FDEs) and the round off error by the computer, the lowest velocities with significance in CFD prediction are expected to be greater than 10^{-4} ft/s.
- Concerns expressed by OPPD and the NRC for this condition led to related experimental work to validate CFD predictions for low velocity conditions. It was shown that FLOW-3D® is capable of predicting low velocities greater than 0.01 ft/s (Reference 21) (See Figure 9 below). Low flow testing was performed in the ALION transport flume to validate Flow-3D's capabilities of predicting low velocities. Flow measurements were conducted for two flow rates: 16.99 and 32.14 gpm. These flow rates result in an average velocity of 0.012 and 0.024 ft/s through the cross-section of the flume, respectively. These average velocities have the same magnitude as the characteristic velocity in the containment pool for no spray conditions. These low flow conditions in the transport flume were also simulated using Flow-3D®. Comparison between measured velocities in the transport flume and predicted velocities using Flow-3D® confirmed the CFD's ability to accurately predict low flow conditions. It takes low velocities and turbulent kinetic energy to transport fine debris. These validated CFD predicted velocities are sufficiently large to transport fine debris.
- The characteristic velocity in the flow region of the containment pool has the magnitude of 0.01 ft/s (see Figure 9 below). The stagnant regions are separated from the sump by the regions where the velocities are less than 0.01 ft/s.

Therefore, it was assumed that no transport of fine debris occurs in pool regions where the predicted velocities are less than 0.01 ft/s and the TKE does not predict high enough turbulence. These regions are considered stagnant regions. Looking at massless particle releases from a break in SG A or B was used along with evaluating the pool velocity 1 inch above the containment floor. (Figure 7) These areas for potential transport were then compared to areas that had sufficient TKE to suspend individual fibers. (Figure 8) Thus, if an area had predicted pool velocity greater than 0.01 ft/sec (which is greater than the settling velocity of most fines) and the TKE was high enough to have suspension (shown in Figure 8 as continuous iso-surfaces), then that area was considered as a fines debris transport area. The flow regions identified in Figure 9 are substantially larger than the continuous yellow iso-surface regions shown in Figure 8. Therefore, this assumption is conservative.

Unqualified Coatings

The majority of unqualified coatings in the FCS containment are located at elevations well above the basement floor at elevation 994'. These coatings, should they fail post-DBA, would fail near the component they were applied to and as such, would fall to the concrete slab floor immediately below that component. As can be seen in Figures 10 and 11 below, the FCS containment is comprised predominantly of concrete slab floors at the upper elevations. Thus, if coatings failed they would most likely reside on the component or near it and not fall through gratings. Also, since FCS will not employ containment spray post-LOCA, there will be no motive force (other than condensation washdown) for sliding or driving failed coatings to subsequent lower elevations. Without spray washdown, there would be no water sheeting action to move coatings towards gratings or openings or stairwells and no significant movement of failed unqualified coatings to lower elevations or ultimately to the containment basement floor. Therefore, the failure of unqualified coatings needs only to be evaluated on the containment basement elevation 994'.

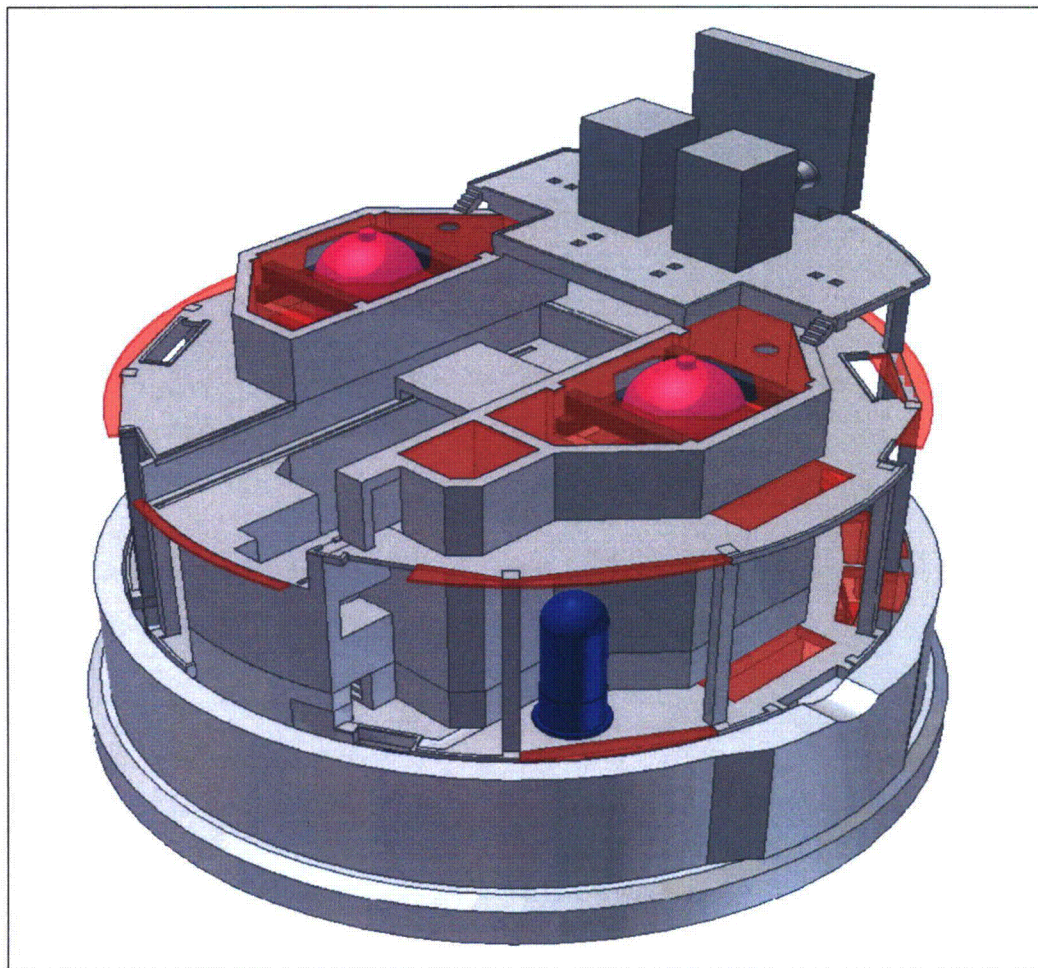


Figure 10
Upper Containment

calculated from the debris generation calculation would be predicted to be at the strainer. The amount of debris in the event of a SBLOCA would then equate to what was calculated from debris generation calculation and shown in Table 17 below.

Table 17
SBLOCA results

Debris Type	Mass or Volume
LDFG (fines)	0.98 ft ³
Cal-Sil (fines)	0.71 ft ³
Unqualified Coatings	22.3 lbm
Qualified Coatings	2 lbm
Particles Latent Debris	40.2 lbm
Fiber Latent Debris	2.2 lbm
Other Latent Debris	37.2 lbm
Stickers, Tape, Labels	71 ft ²
Sand	0 lbm

Table 18 below shows the results of a break at the reactor vessel nozzles, which addresses sand transport.

Table 18
RV Nozzle Break Results

Debris Type	Debris Transport Fraction	Mass or Volume
LDFG (fines)	23%	1.8 ft ³
Stainless Steel RMI	0%	0 ft ²
TempMat [®]	8%	0.9 ft ³
Cal-Sil (fines)	19%	7.8 ft ³
Unqualified Coatings	100%	215.7 lbm
Qualified Coatings	23%	2 lbm
Particles Latent Debris	65%	52 lbm
Fiber Latent Debris	65%	3 lbm
Other Latent Debris	65%	49 lbm
Stickers, Tape, Labels	100%	71 ft ²
Sand (A or B nozzle break)	Varies by break*	121 lbm A side 710 lbm B side

*A break in a penetration that is adjacent to the A SG bay results in sand debris that is blown into the A SG bay, and then subject to transport to the sump strainer. A break in a penetration that is adjacent to the B SG bay results in sand debris that is blown into the B SG bay, and then subject to transport to the sump strainer. A nozzle break on the B SG bay side results in debris that is blown into the bay area that is closest to the sump strainer.

No credit was taken for any debris interceptors at FCS, as they are not installed in containment. Hence, the tables provided above identify the total quantities of each type of debris transported to the strainers for the breaks analyzed.

despite the use of conservative assumptions regarding the approach velocity at the strainer surface.

Prototypical Head Loss Testing for the Strainer

Prototypical head loss testing was conducted using module testing (Reference 26). A module test is a head loss test that uses multiple disk sets to simulate a full size strainer. The debris load and flow rate are scaled to simulate plant conditions.

The test module used for all tests except the LBLOCA chemical precipitant test, consists of 15 strainer plates, which are of the same length and width as the plant strainer plate, which is 48" by 33". A sketch of the test module is shown in Figure 13 below. All of the dimensions of the strainer plates including the perforated plate, wire cloth dimensions and internal framework are the same for the test article as they are for the plant strainer. Any differences between the test and plant strainer are noted below:

- For the test module, the outer surface of the disks at each end of the test module are solid sheet material and not perforated plate/wire cloth. These outer test disk frames are half as thick (1/4") as the inner test disk frame in order to model the flow in the frame cavity that represents flow approaching only from the inner surface of each disk. The test module is mounted on a frame, which is prototypical of the plant configuration.
- The perforated plate thickness for the test module is 0.046" compared with the plant perforated plate thickness of 0.059". This thinner perforated plate was evaluated and shown to be acceptable to handle the expected test conditions without structural damage. This difference has no effect on hydraulic performance.
- The inner cavity diameter is the same for both the test article and plant strainer. The resulting clean head loss from the test article inner cavity will be less than the plant strainer inner cavity clean head loss due to the reduced flow rate and reduced length of the inner cavity in the test. For the clean head loss evaluation, the measured clean head loss from the test is assumed to be due to only the strainer disks and ignores the contribution from the inner cavity. The head loss for the inner cavity is calculated and added to the measured clean head loss to determine a conservative clean head loss for the strainer.

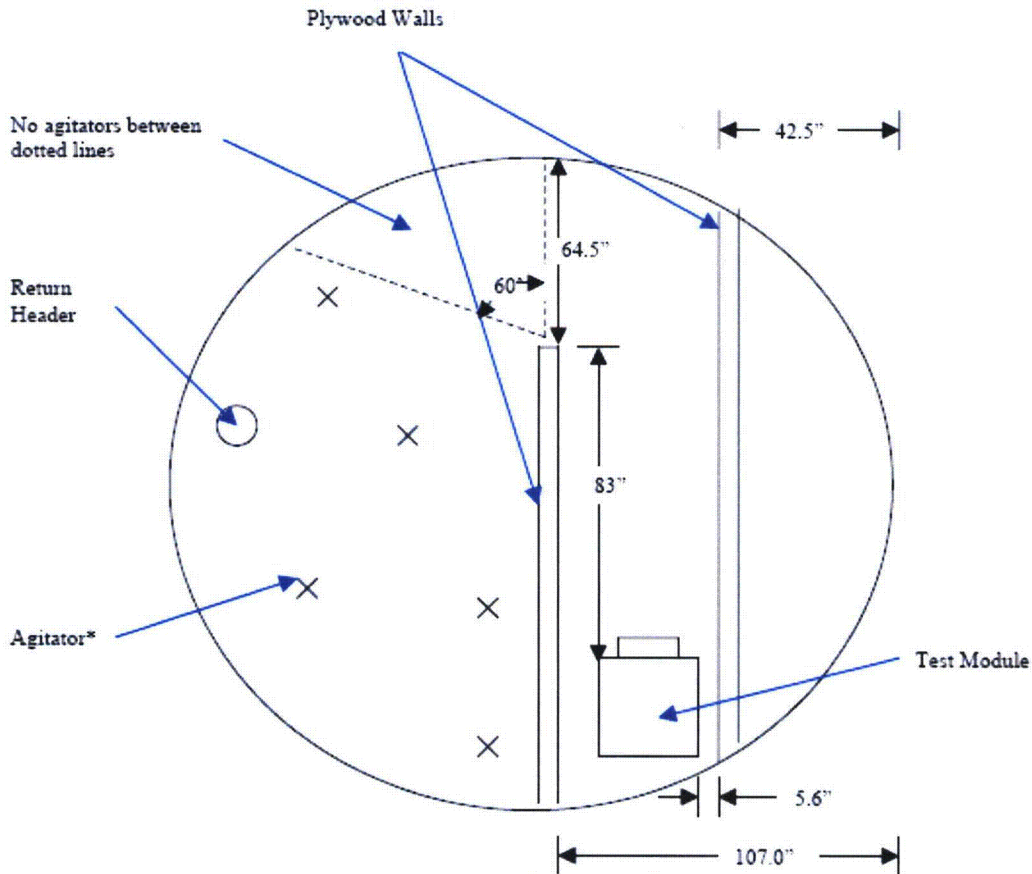


Figure 15
Module Test Configuration (Plan View)

For the SBLOCA, a different test setup was used from the LBLOCA. The small line break location at FCS is located such that the debris transport for Strainer "B" will be bounded by the LBLOCA transport to Strainer "B". The LBLOCA test configuration is conservative for the SBLOCA configuration for Strainer "B" and the LBLOCA debris loads bound the SBLOCA. Therefore, the test results for the LBLOCA which models Strainer "B" will bound the SBLOCA for that strainer.

For Strainer "A" there will be a direct path between the break location and the strainer. Consequently, testing for this strainer did not credit near field settling and was well mixed in front of the strainer. Figure 16 below is a plan view of the test setup for the SBLOCA break scenario.

The following table provides the final results of the prototypical strainer head loss testing.

**Table 19
 Strainer Head Loss Testing¹**

Test Label	Clean Head Loss (in)	Flow Rate at Max Head Loss (gpm)	Maximum Head Loss (in)	Temperature at Max Head Loss (°F)
1M-LBLOCA	0.7	499.4	10.9	94.1
2M-LBLOCA -0.25	0.7	497.2	24.9	96.4
3M-LBLOCA -0.125	0.6	495.7	27.5	97.2
4M-LBLOCA -0.0625	0.6	493.7	19.0	93.4
5M-LBLOCA -FCE (0.125)	0.1	176.8	37.9	96.7
6M-RPT	0.1	261.5	49.6	92.2
7M-RPT	0.2	261.0	0.5	96.1
8M-RPT	0.2	261.3	43.4	96.5
9M-RPT	0.1	263.8	32.8	93.5
10M-SBLOCA -LDFG	0.2	257.9	76.2	94.7
11M-SBLOCA -Jacketed	0.2	258.1	70.0	92.5

¹ Note: Results in Table 19 are not scaled or corrected for instrument inaccuracies.

Table 19a - Plant Head Loss Summary

	Scaled Strainer Head Loss (ft)	Clean Head Loss (ft)	Total Head Loss (ft)	Allowable Head Loss Limit (ft)	Head Loss Margin (ft)
5M-LBLOCA -FCE (0.125)	3.357	0.073	3.430	5.34	1.91
11M-SBLOCA -Jacketed	3.243	0.072	3.315	4.79	1.48

Four (4) LBLOCA tests were performed, with thin bed debris loads and without chemical precipitants, to determine the worst debris load case for head loss. The thin bed debris loads consisted of 0.5, 0.25, 0.125 and 0.0625 inches. The results showed the 0.125 inch thin bed resulted in the worst case for head loss. Based on these results, the 5M-LBLOCA incorporated the debris load from the 3M-LBLOCA-0.125 together with chemical precipitants to obtain the maximum head loss. (5M-LBLOCA-FCE)

For LBLOCA assuming turbulent flow due to bore holes, the plant head loss is proportional to the square of the ratio of the plant debris bed velocity and test debris bed velocity. (A bore hole is the sudden collapse of the debris bed in a localized area, which allows the turbulent flow of water to pass through the debris bed and strainer perforated plate, resulting in reduced head loss.)

The assumption of turbulent flow is conservative as it precludes scaling by kinematic viscosity, which would yield a significantly reduced head loss compared to laminar flow. The strainer head loss at post LBLOCA recirculation conditions was calculated from the testing head loss results using the following scaling equation:

$$\text{Headloss}_{\text{Debris}} = (\text{HeadLoss}_{\text{Test}} - \text{HeadLoss}_{\text{Test.Clean}}) \cdot (\text{Velocity}_{\text{Plant}} / \text{Velocity}_{\text{Test}})^2$$

Where:

HeadlossDebris = Scaled head loss due to the debris
HeadLossTest = Measured maximum head loss from the test
HeadLoss_{Test.Clean} = Measured clean head loss from the test
Velocity_{Plant} = Plant approach velocity
Velocity_{Test} = Test approach velocity

Assuming laminar flow, plant debris head loss is calculated based on the head loss and the differences between plant and test parameters. The parameters are debris bed velocity, viscosity, debris bed thickness and water density. The relationship between plant head loss, test head loss and the difference in plant and test parameters is based on Darcy's law and the resultant equation is shown below in Equation 3.

Equation (3):

$$\text{Headloss}_{\text{Debris}} = (\text{HeadLoss}_{\text{Test}} - \text{HeadLoss}_{\text{Test.Clean}}) \cdot (\text{Viscosity}_{\text{Plant}} / \text{Viscosity}_{\text{Test}}) \cdot (\text{Velocity}_{\text{Plant}} / \text{Velocity}_{\text{Test}}) \cdot (\text{DebrisThickness}_{\text{Plant}} / \text{DebrisThickness}_{\text{Test}}) \cdot (\text{WaterDensity}_{\text{Test}} / \text{WaterDensity}_{\text{Plant}})$$

Where:

HeadlossDebris = Scaled head loss due to the debris
HeadLossTest = Measured maximum head loss from the test
HeadLoss_{Test.Clean} = Measured clean head loss from the test
Viscosity_{Plant} = Plant water dynamic viscosity at 196.6°F
Viscosity_{Test} = Test water dynamic viscosity at 94.5°F
Velocity_{Plant} = Plant approach velocity
Velocity_{Test} = Test approach velocity
DebrisThickness_{Plant} = Plant fiber debris bed thickness
DebrisThickness_{Test} = Test fiber debris bed thickness
WaterDensity_{Plant} = Plant water density at 196.6°F
WaterDensity_{Test} = Plant water density at 94.5°F

During testing for SBLOCA it was evident that bore holes were present in the debris bed. Bore holes cause turbulent flow and will prevent scaling using Equation 3, if there are a significant number of bore holes. If only laminar flow was present, Equation 3 would scale repeatability head loss (HL) of 68.74 inches, at 92.5°F to the theoretical plant head loss at 196.6°F and arrive at the laminar flow head loss of 33.92 inches. To determine the effect of the bore hole on scaling, the 11M-SBLOCA test was run, at approximately 92.5°F, until achieving a maximum head loss of 70.6 inches (corrected for instrumentation accuracy). At this point, the temperature was reduced to 69.7°F and the head loss was allowed to reach a maximum measured head loss of 78.3 inches (corrected for instrumentation accuracy). If the flow had been entirely turbulent the head loss at 69.7°F would have remained approximately the same as the head loss at 92.5°F. Since the head loss did increase, the flow must be a combination of laminar and turbulent flow and would allow for partial scaling, using Equation 4. To determine the scaling

adjustment factor, Equation 3 is used to scale the maximum head loss at 92.5°F (70.6 inches) to the theoretical laminar flow head loss at 69.7°F of 89.82 inches.

The scaling adjustment factor is equal to the ratio of the theoretical laminar flow head loss at 69.7°F (89.82 inches) to the maximum measured head loss at 69.7°F (78.3 inches). The adjustment factor is then applied to the laminar flow head loss at 196.6°F (33.92 inches).

Equation (4):

Plant partially scaled HL at 196.6°F = (Adjust Factor)(Plant laminar flow HL at 196.6°F)

$$\text{Adjust Factor} = \frac{\text{Test theoretical laminar flow HL at } 70^{\circ}\text{F}}{\text{Test maximum measured HL at } 70^{\circ}\text{F}}$$

$$\text{Plant partially scaled HL at } 196.6^{\circ}\text{F} = \frac{(89.82 \text{ in})}{(78.3 \text{ in})} \times 33.92 \text{ in}$$

$$= 38.92 \text{ in} = 3.243 \text{ ft (does not include clean head loss)}$$

Where:

Plant partially scaled HL at 196.6°F: Plant scaled repeatability head loss at 196.6°F using EQ (3), adjusted for turbulent flow.

Plant laminar flow HL at 196.6°F: Plant scaled repeatability head loss at 196.6°F using EQ (3).

Test theoretical laminar flow HL at 69.7°F: Test maximum measured head loss at 92.5°F scaled to head loss at 69.7°F.

Test maximum measured HL at 69.7°F: Test maximum head loss measured at 69.7°F

Maximum Volume of Debris Predicted to Arrive at the Screen

The large break LOCA test discussed in the previous section used a scaled debris load based on the maximum amount of debris transported to the strainer.

Thin Bed Formation

The fiber debris loads for the thin bed test results are based on the amount of fiber to provide a nominal bed thickness on perforated plate of 1/4", 1/8" and 1/16", respectively. The test results demonstrate the ability of the strainer to resist or accommodate the formation of the thin bed.

Basis for the Strainer Design Maximum Head Loss

The basis for the strainer maximum allowable head loss is the lesser of the crush pressure of the strainer or the allowable ECCS head loss. The lesser allowable head loss was determined to be the limiting NPSH margin as determined by different combinations of pumps and plant alignment as discussed in Section 3g below.

Significant Margins and Conservatisms Used in the Head Loss and Vortexing Calculations

The strainer head loss and vortexing were measured using testing. In addition, the possibility of vortex formation at the strainers was evaluated using the conservative

assumption of increasing the approach velocity by a factor of 3, to simulate the increased flow rate near the suction end of the strainer. Testing was performed using a conservatively low containment sump water level, calculated for the present operating conditions, which assume a considerable volume of water hold up in the refueling cavity and containment spray headers. The water level will be higher following implementation of LAR-07-04 (Reference 16). In addition, the head loss testing for the LBLOCA was conducted using the flows associated with 2 HPSI pumps operating on one header in conjunction with the largest debris load which corresponds to the opposite header.

Methodology, Assumptions, and Results for the Clean Strainer Head Loss Calculation

The clean head loss evaluation is based on a combination of strainer head loss and piping head loss. The strainer head loss is composed of the head loss through the individual disc sets and the central channel. The disc set head loss is based on the module test clean head loss results, which are scaled by the square of the ratio of flow velocities. The central channel uses the resistance coefficient K of a straight pipe to calculate the head loss. The piping uses the resistance coefficient K for the individual piping components to determine head loss of the routing. The maximum clean strainer assembly head loss is 0.073 feet for Strainer SI-12B and 0.072 feet for Strainer SI-12A.

Methodology, Assumptions, and Results for the Debris Head Loss Analysis

The strainer debris head loss was measured using testing and was not determined by analysis.

Sump Submergence and Venting

The strainer at FCS is neither partially submerged nor is it vented (i.e., it lacks a complete water seal over its entire surface) for any accident scenario.

Near-Field Settling

Near-field settling was credited for the LBLOCA head-loss testing. The module is placed into a circular tank, which is at least 18 feet in diameter and at least 4 feet high. See Figures 14 and 15 above. Within the test tank, plywood walls were set up as shown in Figure 13 above. This test setup is intended to model the "B" suction strainer location in the FCS containment annulus, because it will pass the higher flow rate post-LOCA as compared to the "A" strainer and thus would experience a higher head loss. In addition, this testing conservatively uses the highest debris load for all analyzed breaks, which occurs in the A SG bay, which is furthest from the strainers. The plywood walls in the test tank represent the containment wall (wall to the right of the test article on Figure 15) and the bioshield wall (wall to the left of the test article on Figure 15). The distance between the walls is established such that, based on the height of water in the tank, the approach velocity of water in ft/sec across the test strainer would be the same in the test as for the plant in order to accurately model debris settling in that area.

Flashing

An assessment of FCS sump strainer potential for void formation was conducted and documented. The assessment was performed with the following conservative assumptions which provide additional margin: the worst case total head loss across the strainer, conservative containment pool area, and the maximum flow rate through the strainer. In addition, the submergence of the strainer was assumed to be only from the post-LOCA pool water level to the top of the strainer. This is conservative since the strainer perforated flow plates are below the top of the strainer, at a greater submergence; hence there is a higher hydrostatic head with the consequential smaller void fraction. The calculations indicate that for fluid temperatures equal to or less than 205°F the void fraction downstream of the ECCS strainer is less than 3% (at 205°F, the void fraction was estimated to be 2.62%, with no credit for containment overpressure). For the maximum calculated fluid temperature of 213°F, a containment overpressure of 5.4 ft water is required to keep the void fraction less than 3%. Long-term sump temperature and containment pressure analyses for various alignments show that only one case results in sump temperatures above 200°F, for a period of time no longer than 4 hours. The ~ 5 ft. overpressure credit to ensure that the void fraction remains below 3%, is consistent with the overpressure required to ensure adequate net positive suction head (NPSH) available for the high pressure safety injection (HPSI) pumps, as described in Reference 16. The credited overpressure is considerably lower than the available overpressure during that time period, which is well above 20 ft.

System response is determined by break size and resulting RCS and containment pressure characteristics. The ECCS original design was such that for a large break LOCA, all safety injection and containment spray pumps were started. Amendment 244 (Reference 57) implemented in November 2006 allowed the disabling of the auto-start feature of one CS pump. In 2004, emergency operating and abnormal operating procedures were revised to secure one HPSI pump prior to or shortly following RAS if all three HPSI pumps are in operation (Reference 56).

LAR-07-04 (Reference 16) was submitted by OPPD in July 2007 and is presently under review by the NRC. LAR-07-04 changes the containment spray actuation logic such that the CS pumps will not start during a LOCA. The new CS system actuation logic will require that both the steam generator low signal (SGLS) and the containment spray actuation signal (CSAS) be initiated before the CS system is actuated. Thus, containment spray will not initiate in response to a LOCA, and for a large-break LOCA, only the HPSI and LPSI pumps will inject water into the core. Upon depletion of water in the SIRWT, and initiation of recirculation, the LPSI pumps are automatically stopped and the HPSI pumps are aligned to take suction from the containment sump.

The basis for the containment spray actuation logic change is to improve the NPSH margin for the HPSI pumps by reducing the head loss and hydraulic resistance through the containment sump strainers when the HPSI pumps are operating in the recirculation mode. (The LPSI pumps are automatically shut off following a RAS.) The enhancement in the NPSH performance will be due to reduced transport of debris to the strainer resulting in a reduction in the pressure drop across the strainer and a reduction in piping head loss. This will provide additional margin for the NPSH available ($NPSH_A$) for the HPSI pumps taking suction from the containment sump, increase the amount of water delivered to the core during the injection phase of a LOCA and will increase the time to the initiation of a RAS.

The maximum flow for Train A (Strainer SI-12B) would be 923 GPM and for Train B (Strainer SI-12A) 479 GPM. The flows are based on the calculations of the system performance during the recirculation phase. The worst-case failure from a flow and NPSH margin standpoint is a failure of a LPSI pump to stop at RAS. This failure would result in minimum NPSH margin and maximum flow through one strainer until such time that the pump could be manually stopped by the operators (approximately 10-15 minutes). Additional CFD evaluations for such a condition have shown that this failure would result (under the worst case condition) in loss of only one strainer train. The remaining train would not be affected and will perform its design function. Therefore, no additional NPSH calculations were performed for this case.

The limiting SBLOCA case for debris transport, is a 3" pressurizer spray line in the vicinity of the strainers, because it provides a direct path to the strainers. The debris produced by the only other line break that can provide a direct path to the strainer (the 4" Pressurizer Code Safety and PORV lines) is bounded by the LBLOCA debris, as

discussed in section 3b. The NPSH margin for the SBLOCA is not limiting because the pump is injecting against a higher RCS pressure and the NPSH required is lower.

NPSH calculations were performed to establish the ECCS and CS pump NPSH margins in the absence of collected debris (i.e., pump NPSH margins were calculated by subtracting the NPSH required, including the head loss across a clean strainer from the NPSH available.) The required NPSH was taken from the curves provided by the pump manufacturer. The NPSH margin in each case was calculated using a sump temperature of 194.7°F, which corresponds to an equivalent 8.99 feet of subcooling, as credited in the USAR. OPPD has previously requested and received NRC approval for crediting up to and including 8.99 feet of containment overpressure to ensure that NPSH requirements of the pumps are satisfied under the most conservative conditions (i.e. possible pump run-out during a LBLOCA) (Reference 39).

The results shown in the Table 20 below represent the NPSH margin calculated after implementation of the proposed containment spray actuation logic change, when only the HPSI pumps (SI-2A, SI-2B and/or SI-2C) are taking suction from the containment sump.

Table 20
Strainer, NPSH and Water Level Margins

Pump	Case	Strainer	Strainer Flow (gpm)	Minimum NPSH margin (ft)	Containment Water level (ft)*
SI-2A	Train A	SI-12B	479	6.06	3.96
SI-2B	Train B	SI-12A	479	5.34	3.96
SI-2C	Train A	SI-12B	479	5.45	3.96
SI-2A	Train A	SI-12B	923	8.30	3.96
SI-2C	Train A	SI-12B	923	7.74	3.96
SI-2B	Train B	SI-12A	471	6.14	3.41

*Note all water levels are based upon the previous spray configuration, which had water holdup in the refueling cavity, containment spray piping, droplets in the air. As such, in the no-spray configuration the containment water level will actually be higher as there will be no holdup in the refueling cavity or in the piping/containment atmosphere.

NPSH calculations were performed using hydraulic models of the system aligned for ECCS sump recirculation per plant procedures. (Reference 37) Different configurations were modeled and the system configuration resulting in the highest flows was used for testing the installed strainers. The configuration resulting in the smallest NPSH margin was used to determine acceptable screen head loss. The calculations use the Proto-Flow model developed to represent the safety injection piping at FCS. The calculations used the FLO-SERIES Pipeline Reports to determine the head loss in the piping system. Fixed hydraulic resistances (K values) provided for specific valves (when available) were used to calculate the flow coefficient (C_v) values and head loss through the components.

the overpressure credit is calculated assuming the maximum allowable head loss across the strainer. No credit for overpressure head is required for hot leg breaks.

The water inventory required to ensure adequate sump pool level and sump pool flow paths was evaluated. The containment water level calculation was developed following walkdowns performed during the 2003 and 2005 RFOs that identified water holdup volumes in the refueling cavity and around the reactor vessel. Flow past the Reactor Pressure Vessel (RPV) flange seal is credited as an alternate flow path. This condition was found acceptable for the current design, however, to minimize water holdup and increase sump pool depth (for increased NPSH margin), a modification to install spacers in the RPV flange was implemented during the 2006 RFO (Reference 18). The water holdup due to the 4-inch diameter drain line in the refueling cavity will no longer be applicable after implementation of LAR-07-04 since the most significant source of water in the refueling cavity was the containment spray water. Installed and planned modifications to plant systems minimized water hold-up, however submergence and available NPSH were calculated using previous configuration and will be conservative following implementation of the water management initiative.

The inputs into the water level calculation are extremely biased toward minimizing the containment water level. The volumes of the tanks contributing to the sump level calculation were assumed to be at their Technical Specifications (TS) minimum required volume, with maximum instrument measurement uncertainty. This is conservative because it results in the minimum volume injected for all water sources into the containment post-LOCA and results in minimum water level in containment. Minimum sump volume is conservative for evaluating submergence of the strainer and therefore potential for vortexing and flashing. It is also conservative for calculating the available NPSH for the pumps taking suction from the sump

The charging pumps would normally operate but no credit is taken for charging pump operation and thus boric acid storage tank (BAST) volume during any LOCA analysis. Therefore, as conservatism, the BASTs were not considered as a source in the water level calculation. (The inclusion of the BAST volume would add approximately 0.3" to the sump pool.) Following installation of the replacement steam generators, RCS volume increased by about 100 ft³, this increase is conservatively omitted from the water level calculation.

The water level calculation (Reference 10) conservatively accounts for the sources of water on the containment floor and for water holdup mechanisms and associated volumes. Determination of the minimum water level accounted for water holdup in the following locations:

- Volume held up as vapor in the containment atmosphere.
- Volume held up on the containment floors above the 994' elevation, including the refueling cavity.
- Volume held up in condensation on heat sink surfaces.

ZOI of 5 D for epoxy was selected based on Reference 4. This testing concluded that a spherical ZOI of 4D is conservative for the "Acceptable" epoxy coatings used at FCS.

For debris generation and transport analysis, 10 micron particles were assumed for "Acceptable" coatings within the 5D ZOI. "Acceptable" coatings outside the 5D ZOI were not assumed to fail.

All "Indeterminate" and "Unacceptable" (Reference 55) coatings are considered to fail. This is consistent with NEI-04-07, which considers all indeterminate and unacceptable coatings as a single category of coating, producing debris of the same characteristics independent of the type of coating when immersed in the post-DBA pool.

Based on the review of Reference 13 unqualified coatings, OPPD could not reduce the failure percentage across the board for all non qualified OEM coatings. However,

3j Screen Modification Package

NRC Guidance

The objective of the screen modification package section is to provide a basic description of the sump screen modification.

- *Provide a description of the major features of the sump screen design modification.*
- *Provide a list of any modifications, such as reroute of piping and other components, relocation of supports, addition of whip restraints and missile shields, etc., necessitated by the sump strainer modifications.*

OPPD Response

The scope of the modification was to perform the hardware changes required to bring FCS into full resolution with GSI-191. This modification, installed during the 2006 RFO, replaced the existing screens for the plant located outside the shield walls on the basement floor of the containment.

The horizontal stacked disk strainers (Figures 18 and 19 below) for FCS Trains A and B consist of a series of 30 horizontally stacked square disks, which are 48" x 33" x 1.22" thick with a 20" O.D. disk spacer in the center. These disks consist of a 1/2" inch frame or internal structure with one perforated plate on each side, 0.059" thick, with 1/16" holes on 7/64" staggered centers with approximately 30% open area and one wire cloth on each side with 0.120" wire diameter, 0.38" opening size and approximately 58% open area. The disks are installed with a 3.0" pitch, which includes a 1.76" nominal gap between adjacent wire cloths. The perforated plate approach velocity is conservatively calculated to be 0.0052 ft/sec for the LBLOCA and 0.0030 ft/sec for the SBLOCA. The strainer configuration is designed to withstand the allowable head loss to 5.3 feet during post-LOCA design conditions.

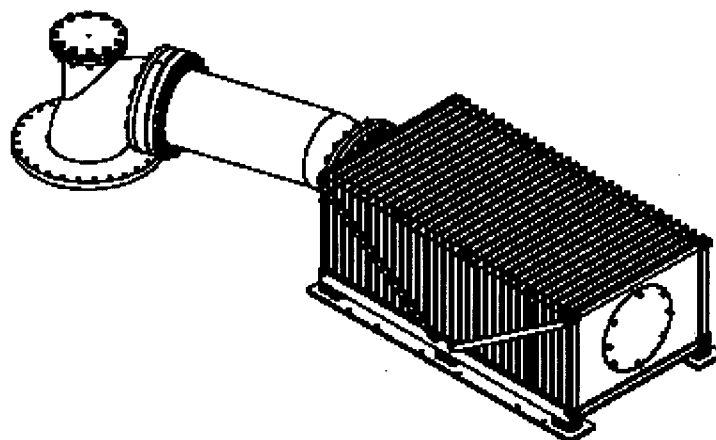


Figure 18
FCS Single Strainer Module

minimum stress ratios are shown in Table 23 and Table 24 below based on the minimum properties and minimum stress allowable. The analysis results show that the ASME code requirements are satisfied for all of the structural components and welds.

Table 23
Stress Ratio Summary for Strainer Components
based on ASME Code Subsection NC

Component	Service Level	Stress Ratio*
Perforated Plates	Design	3.91
Fingers	Design	7.86
Frame and End Cap	Design	13.46
Spacers	Design	7.39
Base	Design	5.10
Outer Rods	Design	3.26
Inner Rods	Design	3.71
Pipe	Design	27.32
Perforated Plates	Level – B	4.30
Fingers	Level – B	8.64
Frame and End Cap	Level – B	14.81
Spacers	Level – B	8.13
Base	Level – B	5.61
Outer Rods	Level – B	3.59
Inner Rods	Level – B	4.08
Pipe	Level – B	30.06
Perforated Plates	Level – D	6.26
Fingers	Level – D	12.57
Frame and End Cap	Level – D	21.53
Spacers	Level – D	11.82
Base	Level – D	8.16
Outer Rods	Level – D	5.22
Inner Rods	Level – D	5.93
Pipe	Level – D	43.71

*Stress Ratio = ASME Stress Limit/Calculated Max. Stress

Table 24
Stress Summary for Welds based on Service level D Load

Weld Location	Weld Stress (psi)	Allowable Stress** (psi)	Stress Ratio*
Perforated Plate to Finger	4,681.42	8,164	1.74
Perforated Plate to Frame	9,272.50	9,342	1.01

*Stress Ratio = ASME Code Stress Limit/Calculated Stress

**Conservative Level A Stress Limits, ASME Code Section III, Subsection ND-3923 at 188 °F

The load due to differential pressure for the sump strainer was determined to be able to withstand a crush pressure of 7 psi (Reference 43).

The test results show that a total of 24.135 gr (grams) of dry fiber bypassed the strainer out of a total of 5084.74 gr (or 0.47%). The total plant strainer fiber bypass was then calculated based on testing results and applying linear scaling of the measured tested fiber bypass. The total bypass consists of the measured fiber bypass plus an additional amount associated with linear extrapolation of the bypass rate at test termination over a 30 day period. This is shown as follows:

Bypass test = Bypass measured + Bypass 30 day

Bypass rate was determined to be 0.12 gr dry fiber in 60 minutes based on measured data.

Therefore,

Bypass 30 day = $(0.12\text{g}/60\text{ min}) \cdot (30\text{ days}) \cdot (24\text{ hours}/\text{day}) \cdot (60\text{ min}/\text{hr})$

Bypass 30 day = 86.40 gr

Bypass measured = 24.135 gr

Bypass test = $24.135\text{ gr} + 86.40\text{ gr} = 110.535\text{ gr}$

This amount of fiber is a small fraction of the initial loading on the strainer. The total bypass fraction for 30 days is therefore,

Bypass fraction = $110.535\text{ gr}/5084.74\text{ gr} = 2.2\%$

The amount of debris that could be anticipated to bypass the plant specific strainer is then calculated:

Bypass test = 110.535 gr = 0.2437 lbm

Area of plant strainer = 516.3 ft²

Aptest = 22.8 ft²

Bypass plant = $(0.2437\text{ gr}) \cdot (516.3\text{ ft}^2/22.8\text{ ft}^2)$

Bypass plant = 5.52 lbm

Based on a micro density of TempMat[®] material of 162 lbm/ft³ the volume of fibers would equate to 0.035 ft³. This is a very small fraction of TempMat[®] material considering the initial load. The actual volume of fibrous debris is quite low in comparison to the amount of debris that was assumed for downstream wear effects (10 ft³). Thus, the actual measured/calculated bypass is approximately a factor of over 200 less than what was evaluated for downstream effects on components, and systems.

The amount of material calculated above was used for determining the chemical effects in the vessel and with fuel using the methodology described in WCAP-16793 (LOCADM calculations) (References 50 and 53). The preliminary calculations indicate with the maximum debris case a fuel clad scale thickness at 37.8 microns (using double the

5. References

1. Calculation FC06985, Revision 1, "Fort Calhoun Station Debris Generation Post-LOCA"
2. Enercon Services Report OPP003-RPT-001 Rev. 1, "Containment Insulation Summary Master 2006 Update"
3. ALION-REP-ALION-2806-01, Revision 3, "Insulation Debris Size Distribution for Use in GSI 191 Resolution"
4. WCAP-16568-P, "Jet Impingement Testing to determine the Zone of Influence (ZOI) for DBA Qualified/Acceptable Coatings, Revision 0, June 2006"
5. Not Used
6. NUREG/CR-6808, "Knowledge Base for the Effect of Debris on Pressurized Water Reactor Emergency Core Cooling Sump Performance," LA UR 03 0880, 2003.
7. LANL Report "Characterization of Latent Debris from Pressurized Water Reactor Containment Buildings", M. Ding et al NEA/NRC Workshop on Debris Impact on Emergency Coolant Recirculation Paper, April 26, 2004.
8. ALION-REP-OPPD-3016-001, Revision 0, "OPPD Calcium Silicate Material Characterization Report (SEM)"
9. ALION-REP-OPPD-3016-002, Revision 0, "Calcium Silicate with Asbestos Material Characterization Report (SEM)"
10. Calculation FC07010, "Calculation of Design Basis Minimum Containment Post-RAS Level"
11. Keeler and Long Report No. 06 0413, "Design Basis Accident Testing Coating Samples from Unit 1 Containment, TXU Comanche Peak SES"
12. Letter from J. Cavallo, Vice President Corrosion Control Consultants and Labs, Inc., dated September 20, 2007
13. EPRI Report No. 1011753, September 2005, for Original Equipment Manufacturers (OEM)
14. Bostelman, Jan and Zigler Gil, "Failed Coatings Debris Characterization, Prepared for BWROG Containment Group Committee, ITS Services, Duke Engineering & Services, August 26, 1998"
15. EPRI Report No. 1014883, "Plant Support Engineering Adhesion Testing of Nuclear Coating Service Level 1 Coatings," August 2007
16. Letter from OPPD (D. J. Bannister) to NRC (Document Control Desk), "Fort Calhoun Station Unit No. 1 License Amendment Request (LAR) Modification of the Containment Spray System Actuation Logic", dated July 30. 2007 (LIC-07-0052)
17. Calculation FC07431, Revision 1, GE Calculation 26A7104, "Suction Strainers Stress Analysis Report"
18. Modification EC 36443, "Install a 3/8" Spacer Under Reactor Seal Ring"
19. Calculation FC07460, Sargent & Lundy Calculation 2005-10600, "GSI 191 Evaluation of the Long Term Downstream Effects of LOCA Generated Debris"
20. ALION-REP-LAB-2352-101, Revision 0, "Test Report: Flow Erosion Testing of Cal-Sil Insulation Debris"

21. ALION-REP-LAB-2352-107, "Measurement of Localized Low Velocities in Transport Flume Testing Report"
22. Calculation FC07248, "OPPD Chemical Product Generation Report"
23. WCAP-16530, "Evaluation of Post-Accident Chemical Effects in Containment Sump Fluids to Support GSI-191"
24. WCAP-16785-NP, "Evaluation of Additional Inputs to the WCAP-16530-NP Chemical Model," May 2007
25. Calculation FC07090, Sargent & Lundy Calculation 2005-08220, Revision 0
26. GEH Document, 26A7408 Rev. 2, Fort Calhoun, "Module Head Loss Testing of Sump Strainers"
27. GEH Document, Deviation Disposition Request, 437004232-004
28. 6898-631-01, "5M-LBLOCA-FCE-Verified"
29. 6898-715-01, "11M-SBLOCA-Jacketed-Verified"
30. GENE-0000-0039-6317-R12, "Design Input Request (DIR) S0100," Rev. 12
31. 0000-0081-2633-R0, "FCS Strainer Air Ingestion Analysis"
32. 234C9215, Rev 4, "ICD, Passive Strainer, 48x33, 30 Disk"
33. Letter from OPPD (H. J. Faulhaber) to NRC (Document Control Desk) "Revised Request for an Extension to the Completion Date for Corrective Actions Taken in Response to Generic Letter 2004-02," dated June 9, 2006 (LIC-06-0067)
34. Letter from OPPD (H. J. Faulhaber) to NRC (Document Control Desk) "Correction to Revised Request for an Extension to the Completion Date for Corrective Actions Taken in Response to Generic Letter 2004-02," dated June 12, 2006 (LIC-06-0069)
35. Letter from OPPD (H. J. Faulhaber) to NRC (Document Control Desk) "Supplement to Revised Request for an Extension to the Completion Date for Corrective Actions Taken in Response to Generic Letter 2004-02," dated June 28, 2006 (LIC-06-0070)
36. WCAP-16851-P, Revision 0, "Florida Power and Light Jet Impingement Testing of Cal-Sil Insulation," dated October 2007
37. Calculation FC07078, "Recirculation Phase System Performance for Safety Injection and Containment Spray Systems"
38. GE Test Report, S0100, Report # 0000-0075-4537, Rev. 2
39. Letter from NRC (L. R. Wharton) to OPPD (S. K. Gambhir) "Fort Calhoun Station, Unit No. 1 – Generic Letter 97-04, Assurance of Sufficient Net Positive Suction Head for Emergency Core Cooling and Containment Heat Removal Pumps" (TAC No. M99992)" dated March 7, 2000 (NRC-00-0031)
40. Letter from NRC (C. Haney) to OPPD (R. T. Ridenoure), "Fort Calhoun Station, Unit No. 1 - Generic Letter 2004-02 Extension Request Approval (TAC No. MD2323)," dated August 14, 2006 (NRC-06-0103)
41. Modification EC37048, "Replacement of Drain Covers"
42. ALION-CAL-OPPD-4089-01, Revision 0, "Fort Calhoun Station Aluminum Walkdown Report"
43. Fort Calhoun Nuclear Station GE-Hitachi "Recirc Sump Strainer Disc Crush Pressure Analysis" (FC07408)